

The Ogooue Fan (offshore Gabon): a modern example of deep-sea fan on a complex slope profile.

Salomé Mignard, University of Bordeaux, UMR CNRS 5805 EPOC.

Thierry Mulder, University of Bordeaux, UMR CNRS 5805 EPOC

Philippe Martinez, University of Bordeaux, UMR CNRS 5805 EPOC

Thierry Garlan, SHOM

Abstract. The effects of changes in slope gradient on deposition processes and architecture have been investigated in different deep-sea systems both in modern and ancient environments. However, the impact of subtle gradient changes ($<0.3^\circ$) on sedimentary processes along deep-sea fans still needs to be clarified. The Ogooue Fan, located in the northeastern part of the Gulf of Guinea, extends over more than 550 km westwards of the Gabonese shelf and passes through the Cameroun Volcanic Line. Here, we present the first study of acoustic data (multibeam echosounder and 3.5 kHz, very-high resolution seismic data) and piston cores covering the deep-sea part of this West African system. This study documents the architecture and sedimentary facies distribution along the fan. Detailed mapping of near-seafloor seismic-reflection data reveals the influence of subtle slope gradient changes ($<0.2^\circ$) along the fan morphology. The overall system corresponds to a well-developed deep-sea fan, fed by the Ogooue River sedimentary load, with tributary canyons, distributary channel-levee complexes and lobes elements. However, variations in the slope gradient due to inherited salt-related structures and the presence of several seamounts, including volcanic islands, result in a topographically complex slope profile including several ramps and steps. In particular, turbidity currents derived from the Gabonese shelf deposit cross several interconnected intraslope basins located on the low gradient segments of the margin ($<0.3^\circ$). On a higher gradient segment of the slope (0.6°), a large mid-system valley developed connecting an intermediate sedimentary basin to the more

distal lobe area. Distribution and thickness of turbidite sands is highly variable along the system. However, turbidite sands are preferentially deposited on the floor of the channel and the most proximal depositional areas. Cores description indicates that the upper parts of the turbidity flows, mainly composed of fine-grained sediments, are found in the most distal depocenters.

Keywords: Ogooue Fan, Gulf of Guinea, complex slope profile, turbidity currents, stepped slope

1 Introduction

Deep-sea fans are depositional sinks that host stratigraphic archives of Earth history and environmental changes (Clift and Gaedicke, 2002; Fildani and Normark, 2004; Covault et al., 2010, 2011), and are also important reservoirs of natural resources (Pettingill and Weimer, 2002). Therefore, considerable attention has been given to the problems of predicting architectures and patterns of sedimentary facies distribution in submarine fans. Early models concerning the morphologies of these systems described submarine fans as cone-like depositional areas across unconfined basin floors of low relief and gentle slope gradient (Shepard and Emery, 1941; Shepard, 1951; Dill et al., 1954; Menard, 1955; Heezen et al., 1959). However, studies of outcrops (Kane et al., 2010) and modern seabed datasets (Stevenson et al., 2013; Kneller, 1995) showed that topographic complexity across the receiving basin can strongly influence the organization of architectural elements of submarine fans (Normark et al., 1983; Piper and Normark, 2009). A wide range of geometries and architectural features due to topographic obstacles has been described in the literature. Among these features are ponded and intra-slope mini-basins due to three-dimensional confinement (Prather, 2003; Prather et al., 2012, 2017; Sylvester et al., 2015) or tortuous corridors created by topographic barriers (Smith, 2004; Hay, 2012). Spatial changes in slope gradients are also important as they cause gravity flows to accelerate or decelerate along the slope (Normark and Piper, 1991; Mulder and Alexander, 2001) allowing the construction of

57 several connected depocenters and sediment bypass areas (Smith, 2004; Deptuck et al.,
58 2012; Hay, 2012). These stepped slopes have been described along modern systems
59 such as the Niger Delta (Jobe et al., 2017), the Gulf of Mexico (Prather et al., 1998,
60 2017) or offshore Angola (Hay, 2012), but also in ancient systems such as the Annot
61 Sandstone Formation (Amy et al., 2007; Salles et al., 2014), the Karoo Basin (Spychala
62 et al., 2015; Brooks et al., 2018) or the Lower Congo basin (Ferry et al., 2005).

63 On stepped slopes where structural deformation is very slow, sediment erosion and
64 deposition are the dominant processes that control the short-term evolution of slope. In
65 these systems, the slope gradient variations play a key role and studies have shown that
66 subtle gradient changes ($<0.3^\circ$) can have an important impact on flow velocity and
67 consequently deep-sea fans organization (e.g. Kneller, 1995; Kane et al., 2010;
68 Stevenson et al., 2013). Even though some of these systems have already been
69 described, the impact of subtle changes in slope gradient on deep-sea fan organization
70 still needs to be better understood in order to extend our knowledge on terrestrial
71 sediments routing and on the potential for reservoir deposits in stepped slope settings .

72 The modern Ogooue Fan provides a new large-scale example of the influence of
73 gradient changes on deep-sea sediment routing. This system, which results from the
74 sediment discharge of the Ogooue River, is the third largest system of the Gulf of Guinea
75 after the Congo and the Niger fans (Séranne and Anka, 2005). However, in contrast to
76 these two systems that have been the focus of many studies (Droz et al., 1996, 2003;
77 Babonneau et al., 2002; Deptuck et al., 2003, 2007), the Quaternary sediments of the
78 Gabon passive margin have not been studied, especially in its deepest parts (Bourgoin
79 et al., 1963; Giresse, 1969; Giresse and Odin, 1973). The regional survey of the area by
80 the SHOM (Service Hydrographique et Océanographique de la Marine) in 2005 and
81 2010, during the OpticCongo and MOCOSÉD cruises, provided the first extensive
82 dataset on the Ogooue deep-sea fan, from the continental shelf to the abyssal plain.

83 The objective of this paper is to document the overall fan morphology, and to link its
84 evolution with the local changes in slope gradients or topographic obstacles present in
85 the depositional area. This study contributes to the understanding of the impact of subtle

slope gradient changes on a whole deep-water system. This study can be used to develop predictive models of sedimentary facies distribution for systems located on stepped slope with low gradient changes ($< 0.5^\circ$) and to better constrain sand deposits.

2 Geological setting

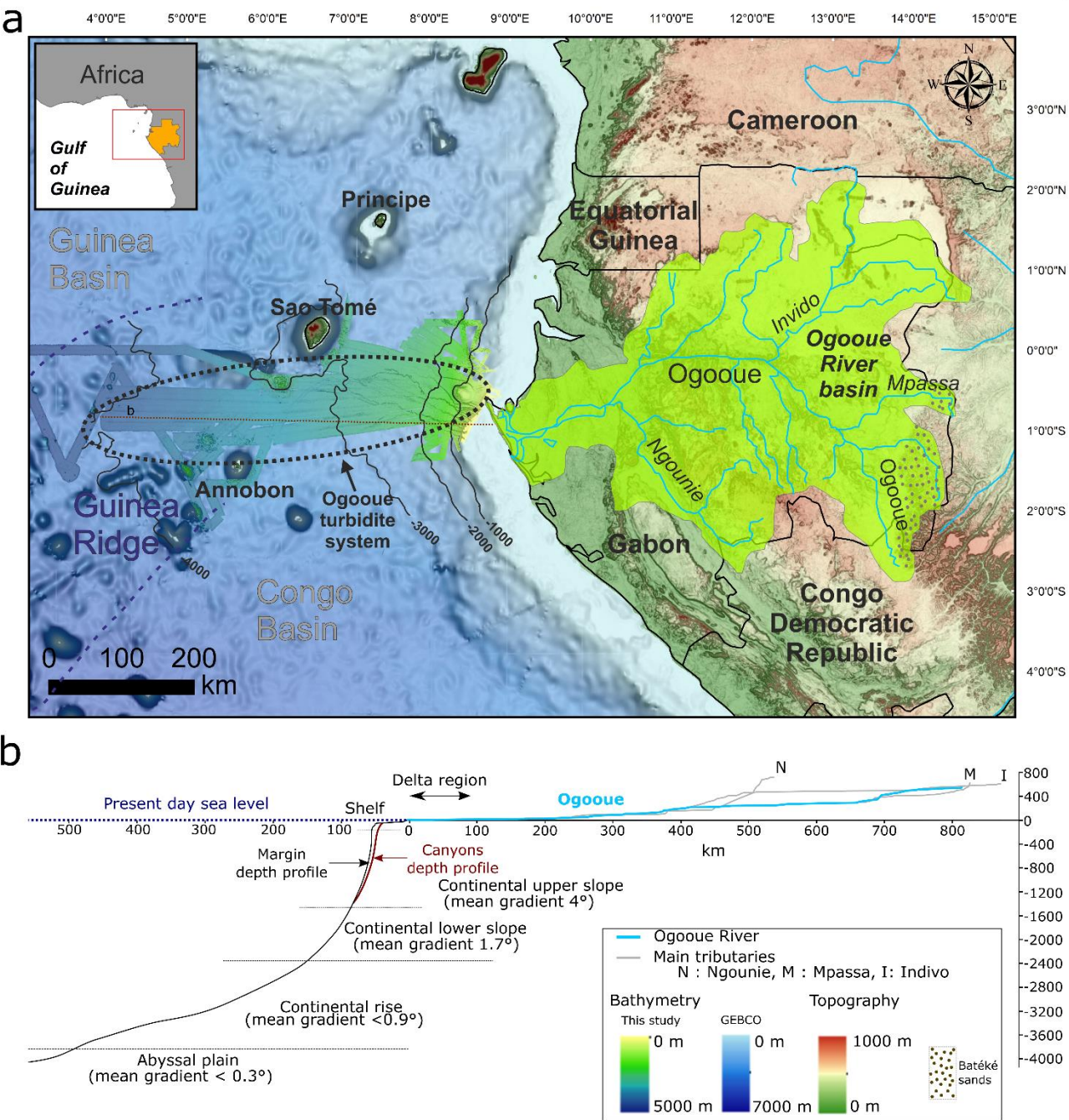


Figure 1: a) The Ogooue sedimentary system from source (river and drainage basin) to sink (Quaternary turbidite fan). b) Channel depth profile of the Ogooue River (blue) and its main tributaries (grey) and mean depth profile along the Gabonese margin.

The continental margin of the Gulf of Guinea formed during the rifting that occurred within Gondwana in Neocomian to lower Aptian times. Syn-rift deposits are buried by mid-late Cretaceous transgressive sedimentary rocks consisting initially of evaporites, which have created salt-related deformations of the margin sediments, followed by platform carbonates (Cameron and White, 1999; Mougamba, 1999; Wonham et al., 2000; Séranne and Anka, 2005). Since the Late Cretaceous, the West African margin has recorded clastic sedimentation fed by the denudation of the African continent (Séranne and Anka, 2005). Different periods of major uplift and canyon incisions occurred from Eocene to Lower Miocene times (Rasmussen, 1996; Wonham et al., 2000; Séranne and Anka, 2005). The sediment depocenters were located basinward of the main rivers, such as the Niger, Congo, Ogooue or Orange River forming vast and thick deep-sea fans (Mougamba, 1999; Séranne and Anka, 2005; Anka et al., 2009).

The Ogooue Fan is located in the northeastern part of the Gulf of Guinea on the Gabonese continental slope. The fan developed on the Guinea Ridge, which separates the two deep Congo and Guinea basins. This region is notably characterized by the presence of several volcanic islands belonging to the Cameroon Volcanic Line (CVL) associated with rocky seamounts (Figure 1a). Geophysical studies of the volcanic line suggest that the volcanic alignment is related to a deep-mantle hot line (Déruelle et al., 2007). All the volcanoes of the CVL have been active for at least 65 Ma (Lee et al., 1994; Déruelle et al., 2007). Ar/Ar dates performed on Sao Tomé and Annobon volcanic rocks proved the activity of these volcanic island over much of the Pleistocene (Lee et al., 1994; Barfod and Fitton, 2014). The MOCOSÉD 2010 cruise revealed that numerous mud volcanoes were associated with the toe of the slopes of the volcanic islands (Garlan et al., 2010). They form small topographic highs on the seafloor (< 20 m high and 100 m in diameter) and show active gas venting (Garlan et al., 2010).

The Quaternary Ogooue Fan extends westwards over 550 km through the CVL. Overall, the modern slope profile is concave upward, similar to other passive margins, e.g.

122 eastern Canada margin, north Brazilian margin (Covault et al., 2012). The mean slope
123 gradient shallows from 7° on the very upper slope to $< 0.3^{\circ}$ in the abyssal plain (Figure
124 1b). The Gabonese continental shelf, which is relatively narrow, can be divided into two
125 sub-parts: the south Gabon margin presenting a SE-NW orientation and the north Gabon
126 margin presenting a SW-NE orientation. The southern part of the margin is
127 characterized by the presence of numerous parallel straight gullies oriented
128 perpendicular to the slope (Séranne and Nzé Abeigne, 1999; Lonergan et al., 2013). On
129 the north Gabon margin, the area located between $1^{\circ}00' S$ and the Mandji Island is
130 incised by several canyons that belong to the modern Ogooue Fan (Figure 2a). North of
131 the Mandji Island, the seafloor reveals numerous isolated pockmarks as well as sinuous
132 trains of pockmarks. These features are interpreted as the results of fluid migration from
133 shallow buried channels (Gay et al., 2003; Pilcher and Argent, 2007).

134 The Ogooue Fan is supplied by the sedimentary load of the Ogooue River, which is third
135 largest African freshwater source in the Atlantic Ocean (Mahé et al., 1990). Despite the
136 relatively small size of the Ogooue River basin (215,000 km²), the river mean annual
137 discharge reaches 4,700 m³/s due to the wet equatorial climate (Lerique et al., 1983;
138 Mahé et al., 1990). The Ogooue River flows on a low slope gradient in a drainage basin
139 covered essentially with thick lateritic soils that developed over the Congo craton and
140 Proterozoic formations related to Precambrian orogenic belts (Séranne et al., 2008). The
141 estuary area includes several lakes which trap coarse sediments (Figure 1b) (Lerique et
142 al., 1983) and contribute to the dominant muddy composition of the particle load of the
143 Ogooue River that is estimated between 1 and 10 M t/yr. (Syvitski et al., 2005). The
144 limited portion of sand particles in the river originates mainly from the erosion of the
145 poorly lithified Batéké Sands located on a 550-750 m high perched plateau that forms
146 the easternmost boundary of the Ogooue watershed (Séranne et al., 2008) (Figure 1a).
147 On the shelf, recent fluvial deposits consist of fine-grained sediments deposited at the
148 mouth of the Ogooue River (Giresse and Odin, 1973). The wave conditions on the
149 Gabonese coast are characterized by a predominant direction from South to South-West.
150 Reflection of these southwesterly swells causes coastal sediments to be transported

151 northward (Biscara et al., 2013). Sedimentary transport linked to longshore drift ranges
152 between 300,000 m³/yr. and 400,000 m³/yr. (Bourgoin et al., 1963) and is responsible
153 for the formation of the Mandji Island, a sandy spit 50 km long located on the northern
154 end of the Ogooue Delta (Figure 3). Except for the Cape Lopez Canyon, located just
155 west of the Mandji Island with the canyon head in only 5 m water depth (Biscara et al.,
156 2013), the Ogooue Fan is disconnected from the Ogooue Delta during the present-day
157 high sea-level (Figure 3).

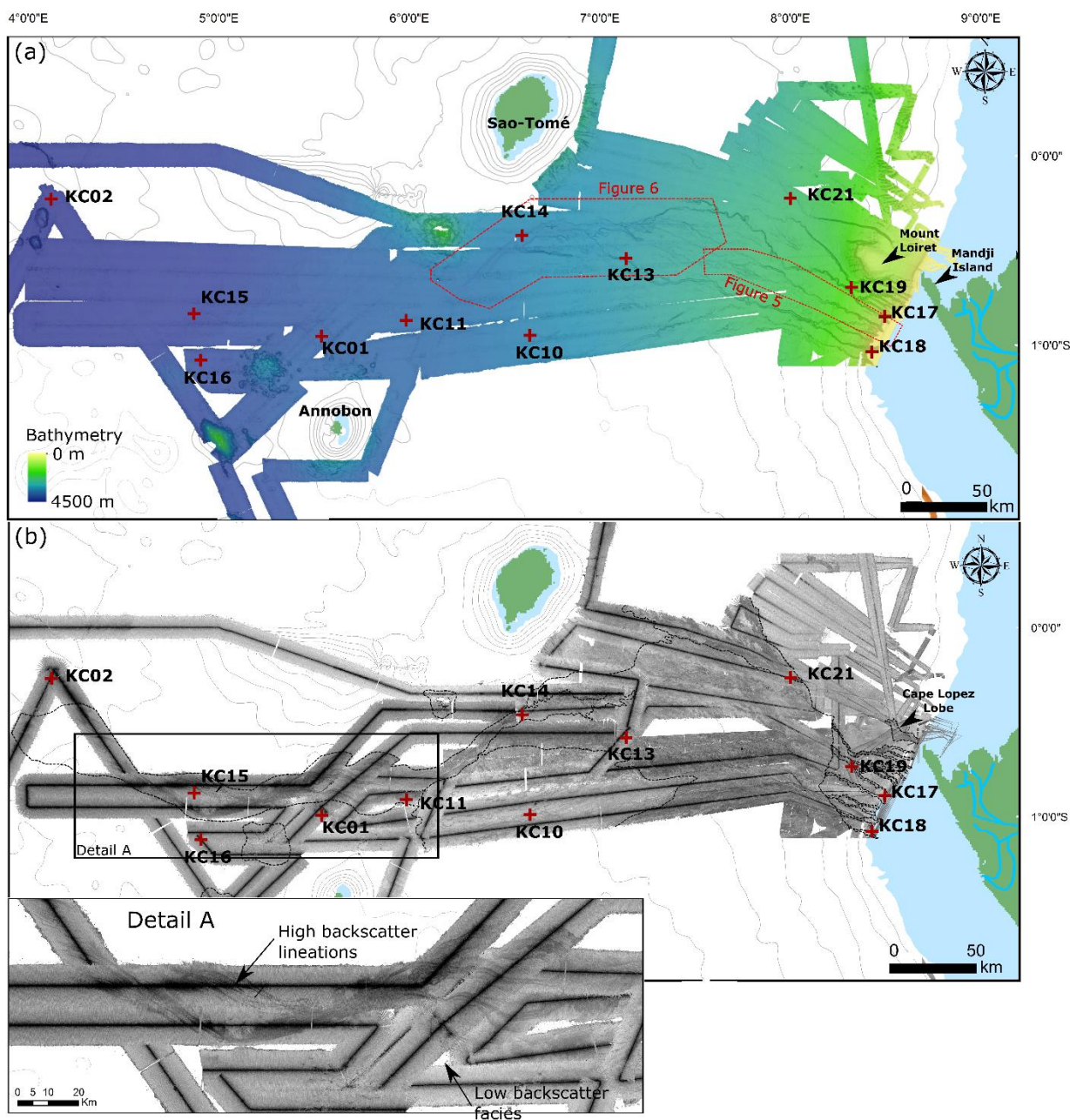


Figure 2: (a) Detailed bathymetric map of the Ogooue Fan, based on the multibeam echosounder data of the Optic Congo2005 and MOCOSD2010 surveys. (b) Acoustic imagery of the Ogooue Fan (high backscatter: dark tones; low backscatter: light tones). Detail A: close-up of the deepest part of the Ogooue Fan. Red crosses: location of the studied cores.

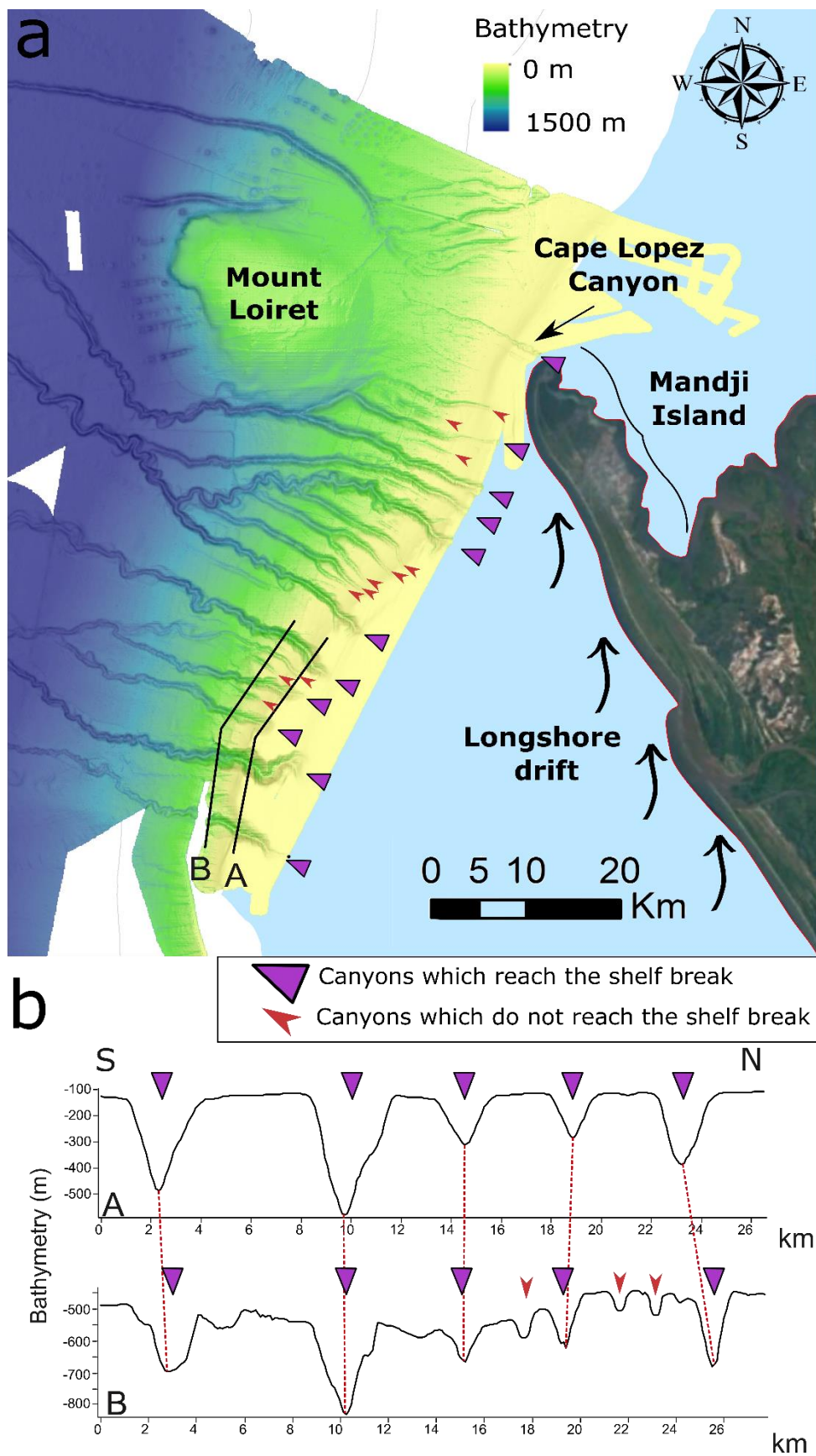


Figure 3: a) Close-up view of the Gabon shelf and canyons ramp. Bathymetry is from the Optic Congo2005 and MOCOSSED2010 surveys, satellite view is from Google Earth. b) Two bathymetric profiles across the canyons showing the two types of canyons which are present along the Gabonese slope.

167 3 Material and method

168 The bathymetry and acoustic imagery of the studied area result from the multibeam
169 echosounder (Seabat 7150) surveys conducted onboard the R/V “*Pourquoi Pas?*” and
170 “*Beautemps-Beaupré*” during the MOCOSSED 2010 and OpticCongo 2005 cruises
171 (Mouscardes, 2005; Guillou, 2010) (Figure 2). The multibeam backscatter data (Figure
172 2b) have been used to characterize the distribution of sedimentary facies along the
173 margin. Changes in the backscatter values correspond to variations in the nature, the
174 texture and the state of sediments and/or the seafloor morphology (Unterseh, 1999;
175 Hanquiez et al., 2007). On the multibeam echosounder images, lighter areas indicate
176 low acoustic backscatter and darker areas indicate high backscatter. Five main
177 backscatter types are identified on the basis of backscatter values and homogeneity
178 (Figure 4). Facies A is a homogeneous low backscatter facies, Facies B is a low
179 backscatter heterogeneous facies, and Facies C is a medium backscatter facies
180 characterized by the presence of numerous higher backscatter patches. Facies D and E
181 are high and very high backscatter facies, respectively. High backscatter lineations are
182 present within Facies D.

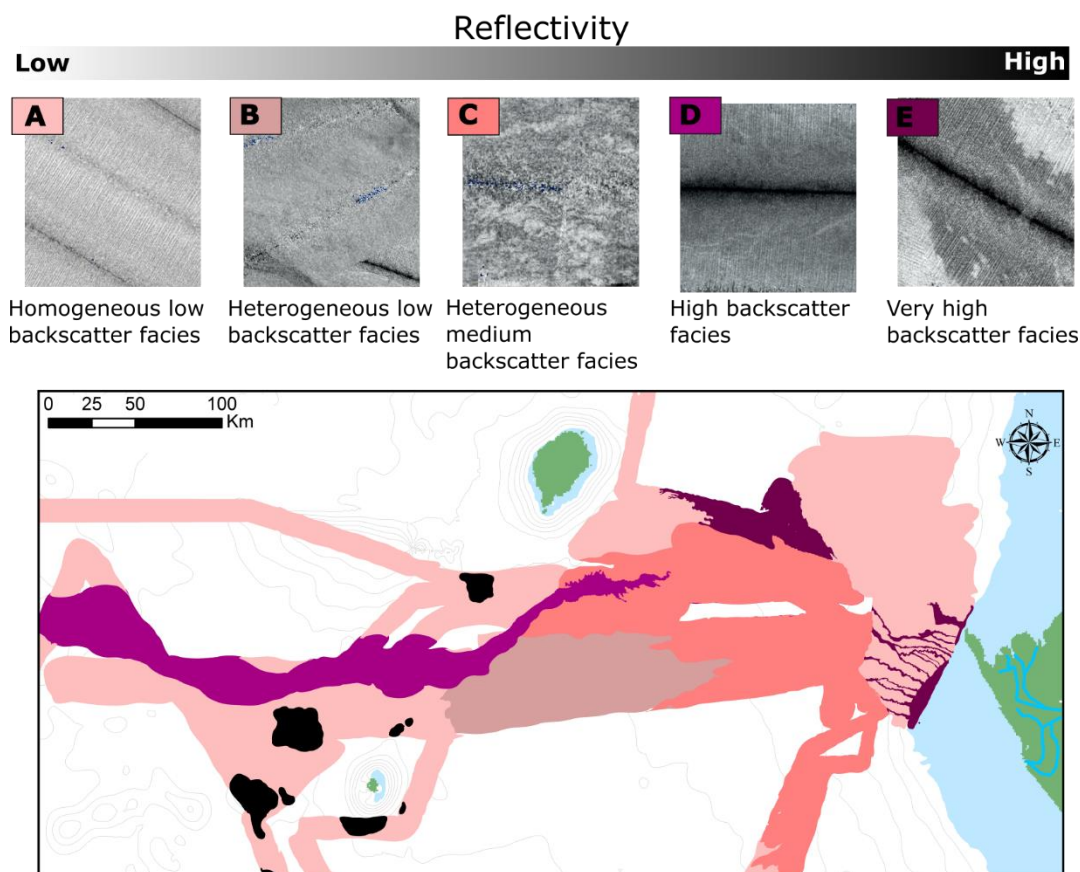


Figure 4: Reflectivity facies map of the Ogooue Fan showing the five main backscatter facies.

A total of four thousand five hundred km of 3.5 kHz seismic lines were collected in the area of the Ogooue Fan during the MOCOSSED 2010 cruise and 470 km during the Optic Congo 2005 cruise (iXblue ECHOES 3500 T7). These data were used to analyze the near-surface deposits. The dataset covers the shelf edge, the slope and the abyssal plain. In this study, the 3.5 kHz echofacies have been classified according to Damuth's methodology (Damuth, 1975, 1980a; Damuth and Hayes, 1977) based on acoustic penetration and continuity of bottom and sub-bottom reflection horizons, micro-topography of the seafloor and presence of internal structures.

The twelve Küllenberg cores presented here were collected during the cruise MOCOSSED 2010. Five of these cores have already been presented in Mignard et al. (2017) (Table 1). Visual descriptions of the cores distinguished the dominant grain size (clay, silty clay, silt, and fine sand) and vertical successions of sedimentary facies. Thin slabs were collected for each split core section and X-ray radiographed using a SCOPIX

digital X-ray imaging system (Migeon et al., 1998). Subsamples were regularly taken in order to measure carbonate content using a gasometric calcimeter and grain size using a Malvern Mastersizer S.

Table 1: Characteristics of the twelve studied cores (MOCOSED 2010 cruise).

| Core | Depth (m) | Latitude | Longitude | Length (m) |
|------|-----------|--------------|---------------|------------|
| KC01 | 3504 | 00°57,010' S | 005°31,806' E | 12,96 |
| KC02 | 4109 | 00°13,525' S | 004°07,620' E | 12,76 |
| KC10 | 3148 | 00°56,666' S | 006°39,809' E | 11,54 |
| KC11 | 3372 | 00°52,008' S | 006°00,008' E | 9,92 |
| KC13 | 2852 | 00°32,508' S | 007°08,589' E | 7,62 |
| KC14 | 3140 | 00°25,010' S | 006°36,006' E | 11,34 |
| KC15 | 3850 | 00°49,996' S | 004°50,009' E | 12,01 |
| KC16 | 3738 | 01°05,003' S | 004°52,010' E | 11,48 |
| KC17 | 565 | 00°51,188' S | 008°29,377' E | 8,20 |
| KC18 | 366 | 01°01,940' S | 008°25,409' E | 7,99 |
| KC19 | 1610 | 00°41,593' S | 008°18,592' E | 10,03 |
| KC21 | 2347 | 00°13,004' S | 008°00,011' E | 11,81 |

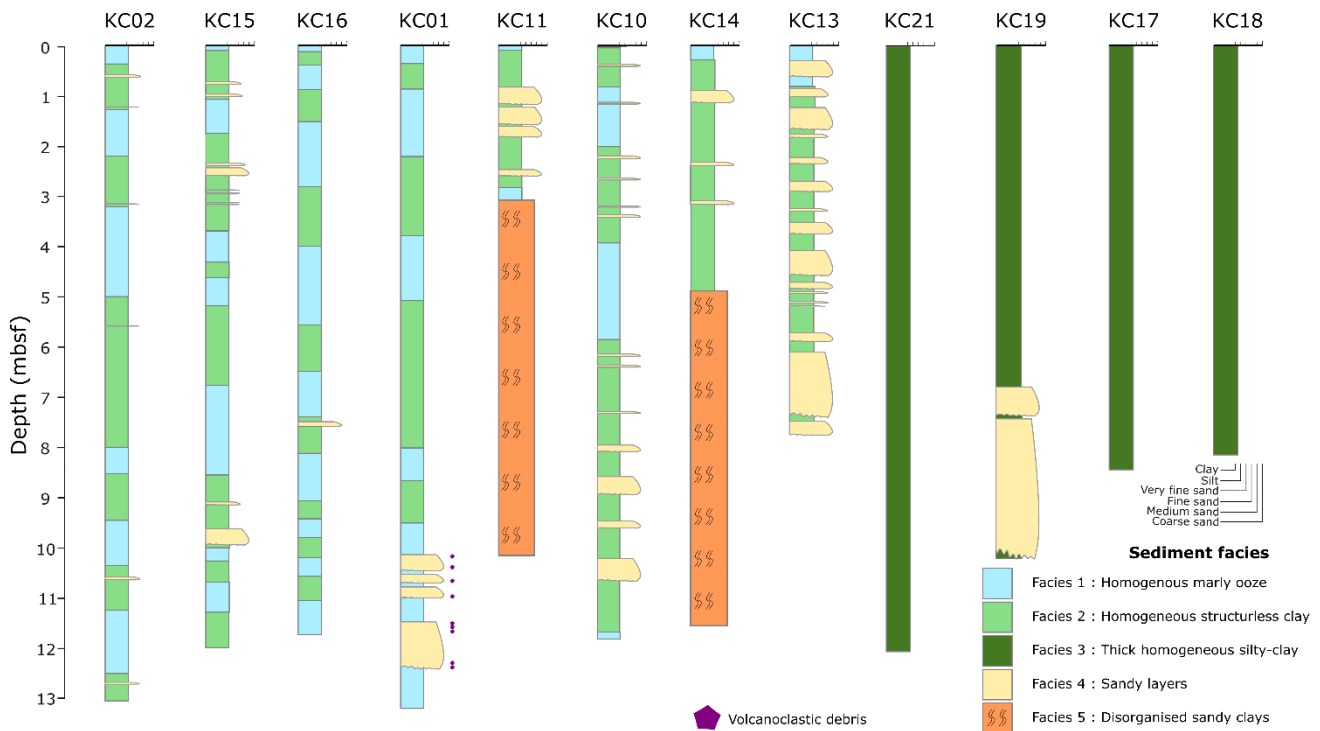


Figure 5: Sedimentological core logs from the Ogooue Fan, showing grain-size variation, lithology and bed thickness (locations of cores are presented in Figure 2).

4 Results

4.1 Sedimentary facies

The classification in five sedimentary facies used here is based on photography and X-ray imagery, grain size analyses and CaCO_3 content (Figure 5, Table 2). Interpretation of these facies is based on the comparison with previous sedimentary facies classifications such as Stow and Piper (1984); Pickering et al. (1986) and Normark and Damuth (1997).

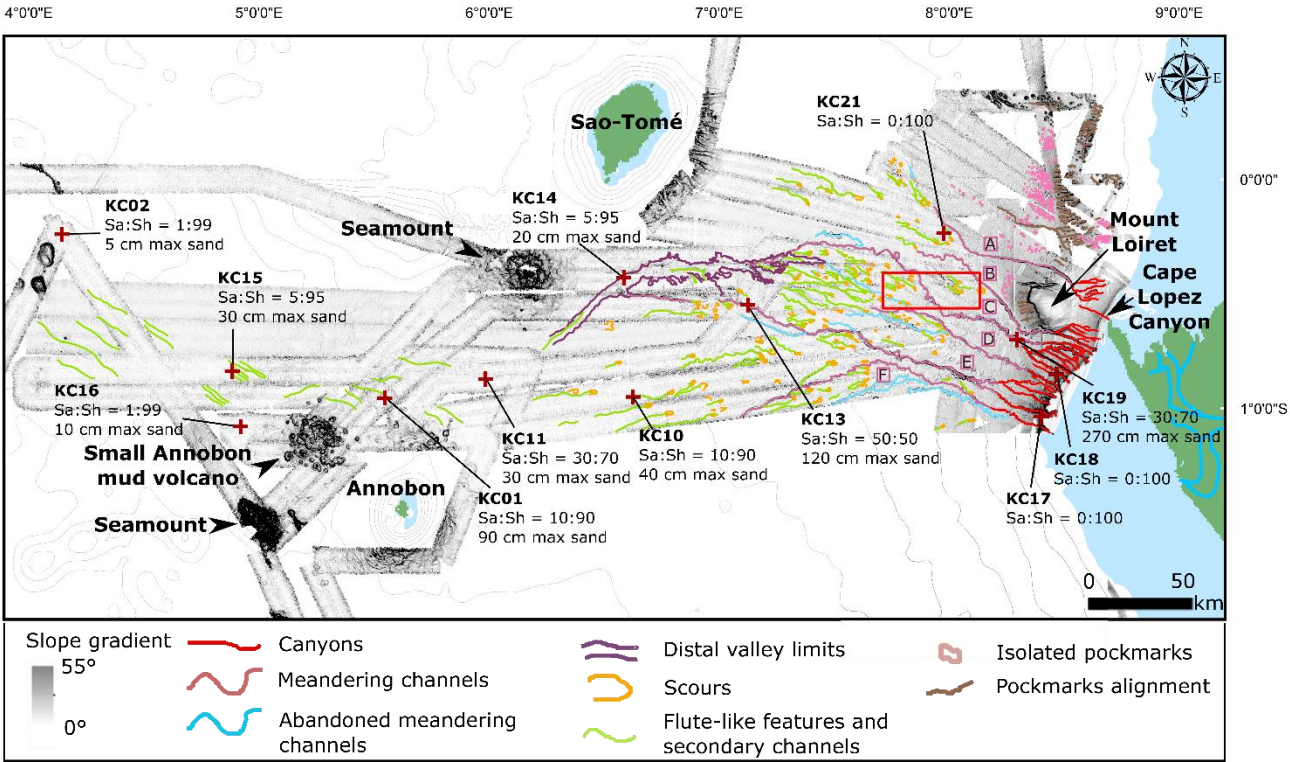
Table 2: Sedimentary facies characteristics.

| Facies | Name | Structure | Color | Mean grain size | CaCO_3 content | Grains | Deposition process | Remarks |
|--------|--------------------------------------|-----------|-------------|------------------|-------------------------|---|------------------------|--|
| 1 | Homogenous, structureless marly ooze | Massive | Light beige | 15 μm | 40-60 % | High concentration of planktonic foraminifers | Pelagic drape deposit; | This facies forms the modern seafloor of the deepest part of the Ogooue Fan and is |

| | | | | | | | | |
|---|--------------------------------------|--|---------------|-----------|-----------------|---|--|--|
| | | | | | | | | observed in most of the core tops. |
| 2 | Homogenous, structureless clay | Massive | Dark brown | 15 µm | <30% | | Hemipelagic drape deposits | |
| 3 | <i>Thick, homogeneous silty-clay</i> | Massive | Dark brown | 40 µm | <10% | high concentration of quartz and mica grains and plant debris | Deposition of the fine-grained suspended load coming from the Ogooue River and flowing down the slope or belonging to the flow tops of the turbidity currents. | |
| 4 | <i>Silty to sandy layers</i> | Massive or presenting ripple cross laminations or parallel laminations | Grey to beige | 60-120 µm | Highly variable | Composed of quartz and mica grains or foraminifers, some sand beds are highly enriched in organic debris (Mignard et al., 2017) | Deposited by turbidity currents initiated on the Gabonese continental shelf. | Four beds sampled at the base of core KC01 present a high concentration of volcanoclastic debris, such particles are completely absent in all the other sandy beds (Figure 5) sandy beds. This specific composition and the particular location of the core both suggest that these sequences originate from the nearby Annobon volcanic island. |
| 5 | <i>Disorganized sandy clays</i> | Deformed or chaotic clay with deformed or folded silty | | | Highly variable | Numerous quartz grains and rare plant debris | Slump deposit or debrite | |

217

218 **4.2 Fan morphology**



219

220 **Figure 6: Interpreted gradient-shaded map of the Ogooue Fan showing the main features of the fan. A, B, C, D, E**
221 **and F are the six main channels discussed in the text. The sand/shale ratio of the cores are shown (Sa:Sh) as well as**
222 **the maximum sand-bed thickness in each core (max sand). A close-up view of the red rectangle is presented in**
223 **Figure 8.**

224 Analysis of the seafloor data (bathymetry and acoustic imagery) reveals the different
225 domains of the Ogooue sedimentary system and the different architectural features of
226 the Ogooue Fan (Figure 6).

227 The Gabon continental shelf is relatively narrow, decreasing in width from 60 to 5 km
228 toward the Mandji Island (Figure 3). The slope is characterized by two main topographic
229 features: (1) the Mount Loiret, a guyot located just west of the Manji Island, which
230 forms a bathymetric obstacle on the upper slope and (2) a ramp of several tributary
231 canyons located south of the Mount Loiret (Figure 3). This ramp is composed of several
232 wide and deep canyons (several hundreds of meters deep and 2-3 km wide near the
233 canyons head), with a “V-shape” morphology and which heads reach the shelf break.

234 Several thinner and shallower incisions are located between these deep canyons. They
235 are less than 100 m deep and 1 km wide and their heads are located between 200 and
236 400 m water depth (Figure 3). The continental shelf and the slope present low
237 backscatter values except for the canyons, which correspond to very high backscatter
238 value (Figure 4).

239 The transition between the continental slope and the continental rise, between 1,200 and
240 1,500 m water depth, is marked by a decrease in the slope gradient from a mean value
241 of 2.3° to 0.9° . At this water depth, several canyons merge to form five sinuous channels
242 (B to F in Figure 6). These channels appear with higher backscatter value than the
243 surrounding seafloor (Figure 4). These sinuous subparallel channel-levees complexes
244 extend down to 2,200 m water depth with a general course oriented toward the north-
245 west (Figure 6 and 7). At 2,200 m water depth, the southernmost channel (channel F in
246 Figure 6) deviates its path toward the south-west.

247 The sinuosity of these channels decreases westward. Channel D sinuosity has been
248 calculated over 2 km long segments (Figure 7C). It is less than 1.1 along the first 13 km
249 corresponding to the canyon part. From 13 to 40 km the mean sinuosity is 1.4 and then
250 decreases to less than 1.2 between 40 to 90 km from the head. Finally, the most distal
251 part of the channel, from 90 km from the head, is very straight with a sinuosity index
252 lower than 1.1 (Figure 7C).

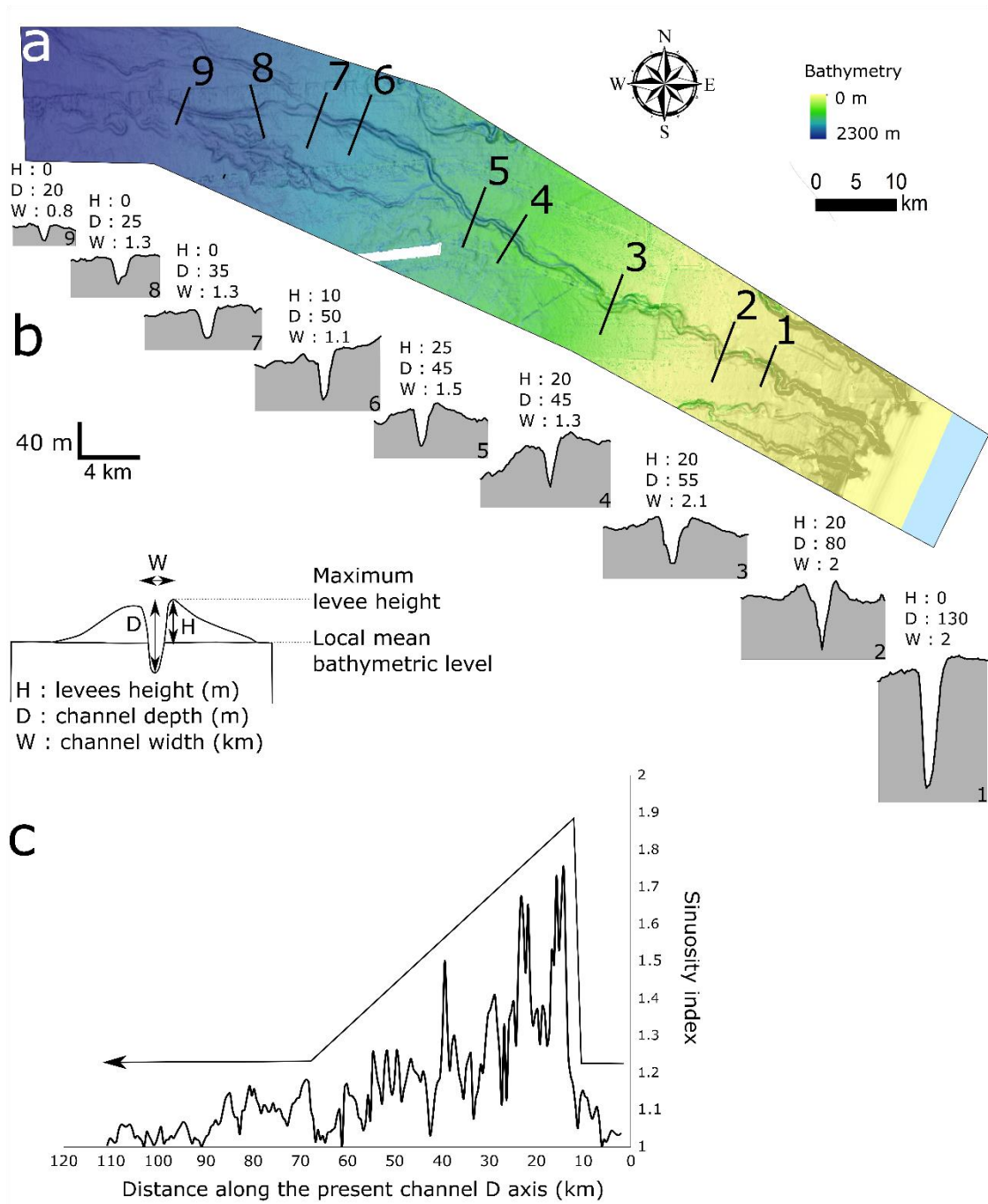


Figure 7: a) Detailed bathymetric map of channel D (location in Figure 2) b) serial bathymetric profiles showing the evolution of the channel-levees along the slope and c) sinuosity down the channel D measured along 2 km channel segments.

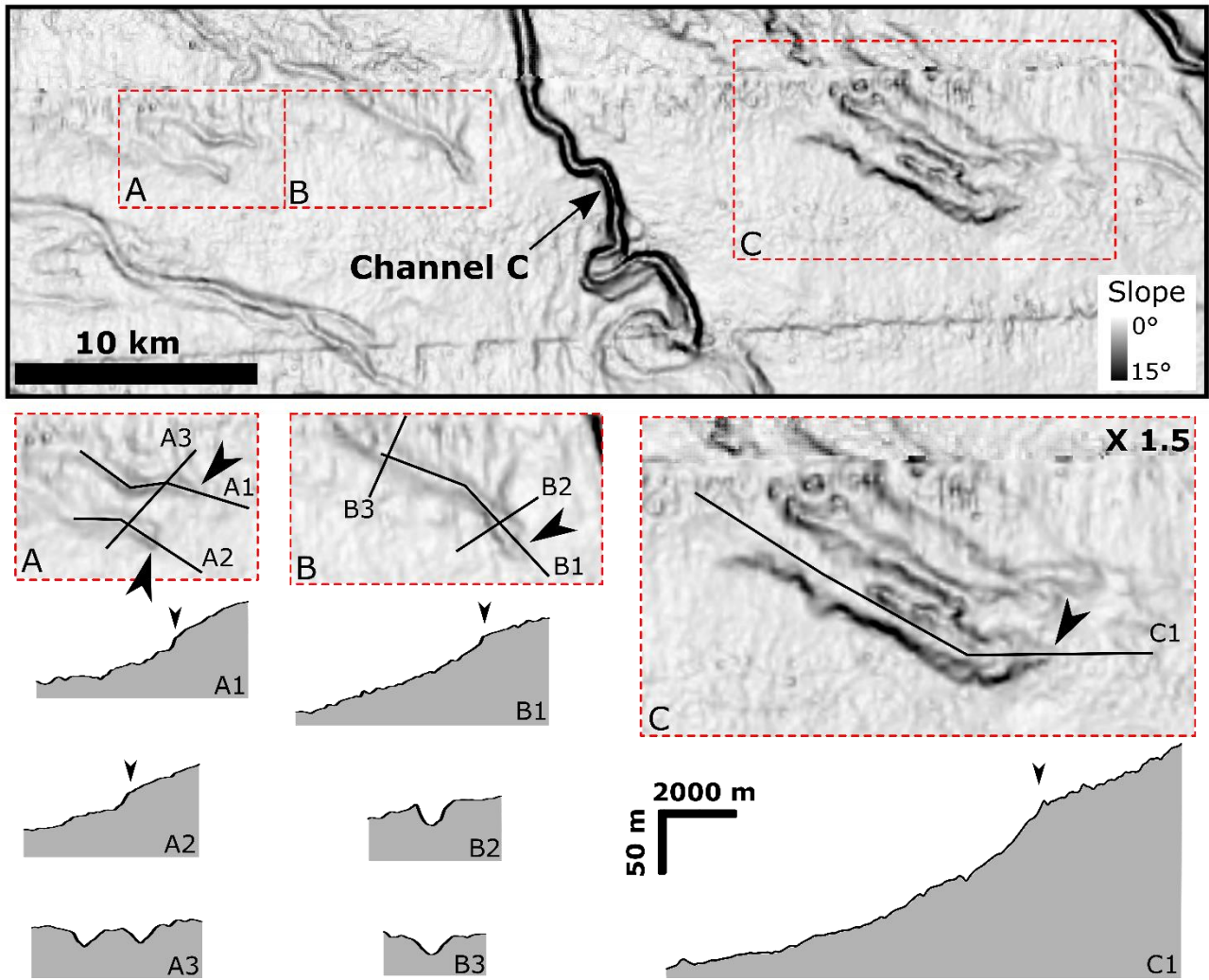
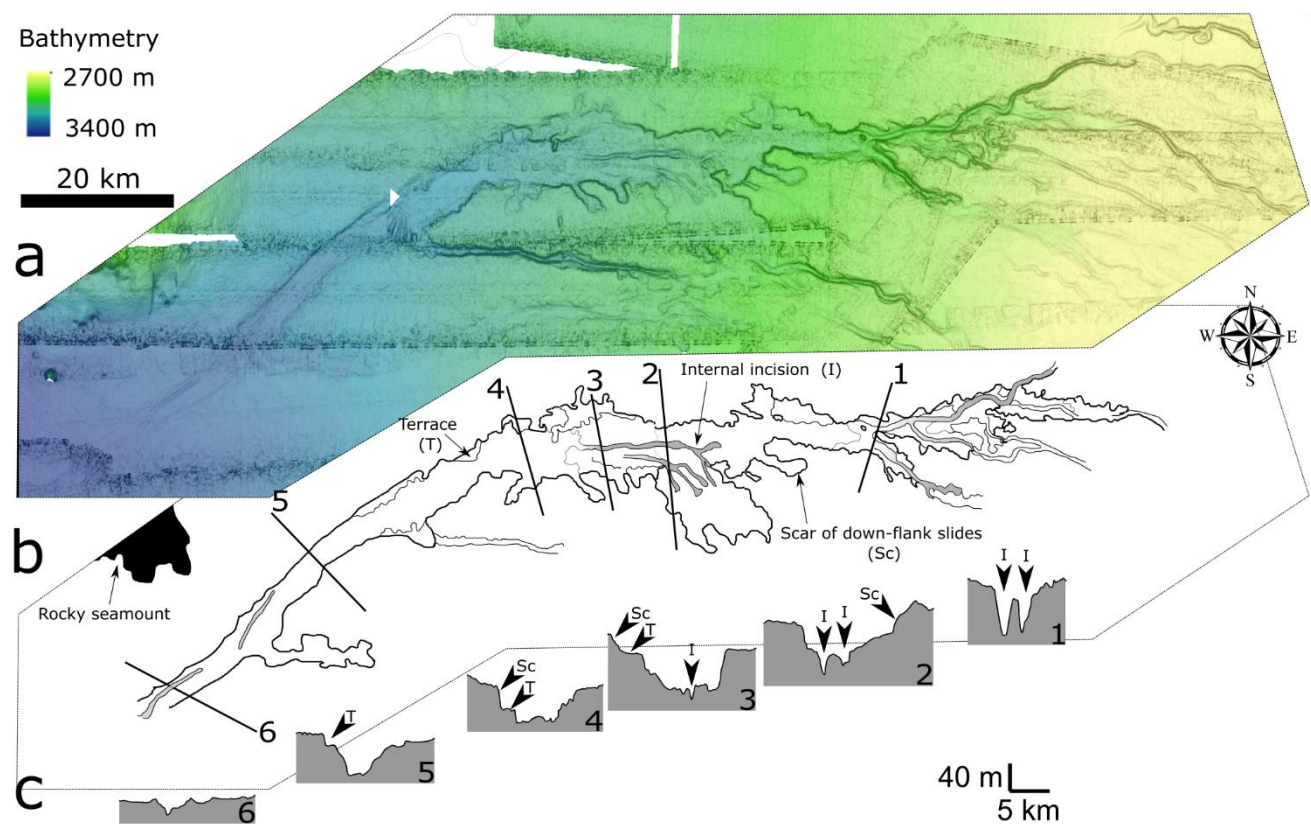


Figure 8: Close-up view of the gradient-shaded map showing erosional lineations (A and B) and amalgamated scours (C) in the central part of the system (location in Figure 6).

Downslope, in the central part of the system, the seafloor located between 2,200 m and 2,500 m water depth presents numerous erosional features including scours, lineations and smaller, subsidiary channels, corresponding to channels with no headward connection with an obvious feeder system according to Masson et al. (1995) (Figure 8). These erosional features appear on a very gentle slope area (0.3°) characterized by a heterogeneous medium backscatter facies (Figure 4). At 2,500 m water depth, just south of the Sao-Tomé Island, the head of a large, 100 km long, mid-system valley appears (Figure 9). This valley can be subdivided in two parts of approximately equal length with two different orientations. The upper part of the valley is oriented E-W, whereas the lower part is oriented NE-SW. This direction change is due to the presence of a rocky seamount located north of the valley and which deflects its course. The upper part

271 of the valley is up to 15 km wide with numerous erosional scars and terraces on its
272 flanks. The valley bottom is characterized by very high backscatter value and small
273 internal erosion channels. Downstream, the valley becomes narrower with a “U” shape
274 (Figure 9, profile 5). Its flanks appear regular with no scar of down-flank mass deposits.
275 The depth of the valley decreases from 60 m in its central part to only 10 m near its
276 mouth. The area located south of the mid-system valley is characterized by a
277 heterogeneous low-backscatter facies. Some erosional features and subsidiary channels
278 are present but scarce.



279
280 **Figure 9: (a) Detailed bathymetric map of the mid-system valley of the Ogooue Fan between 2,700 and 3,400 m**
281 **water depth; (b) Interpretation of the main morphological features of the valley; (c) Six transverse profiles of the**
282 **mid-system valley extracted from the bathymetry data (Sc: scar of down-flank slides, I: internal incision, T;**
283 **Terrace).**

284 West of the mid-system valley outlet, the seafloor is very flat and shows only subtle
285 morphological variations except for local seamounts. Few channel-like, narrow
286 elongated depressions (maximum 10 m deep) presenting high backscatter values can be
287 identified. These lineations are restricted to a long tongue of high backscatter at the
288 mouth of the valley (Figure 2b, Detail A). This tongue is globally oriented E-W at the

289 exit of the mid-system valley and then deflects toward the NW at 3,700 m water depth,
290 following the steepest slope.

291 North of Mount Loiret, the upper slope presents a lower slope gradient compared to the
292 south part and is characterized by the presence of numerous linear pockmark trains on
293 the upper part and pockmarks fields on the lower part. This whole area has a very low
294 and homogeneous reflectivity. Trace of active sedimentation on this part of the margin
295 is only visible in association with the Cape Lopez Canyon (Figure 3). Cape Lopez
296 Canyon terminates at 650 m water depth at an abrupt decrease in slope gradient (from
297 more than 1.7° to 0.6°) caused by the presence of Mount Loiret (Figure 10). This canyon
298 is associated with a small intraslope lobe located just north-east of the Mount Loiret and
299 referred as the Cape Lopez Lobe (Figure 10) (Biscara et al., 2011). This northern system
300 continues basinward with Channel A, the head of which is located in the vicinity of the
301 Cape Lopez Lobe. At 2,200 m water depth, Channel A ends and its mouth is associated
302 on the backscatter map with a fan-shaped area of very-high reflectivity, which is
303 associated with some subsidiary channels and erosional marks (Figure 4).

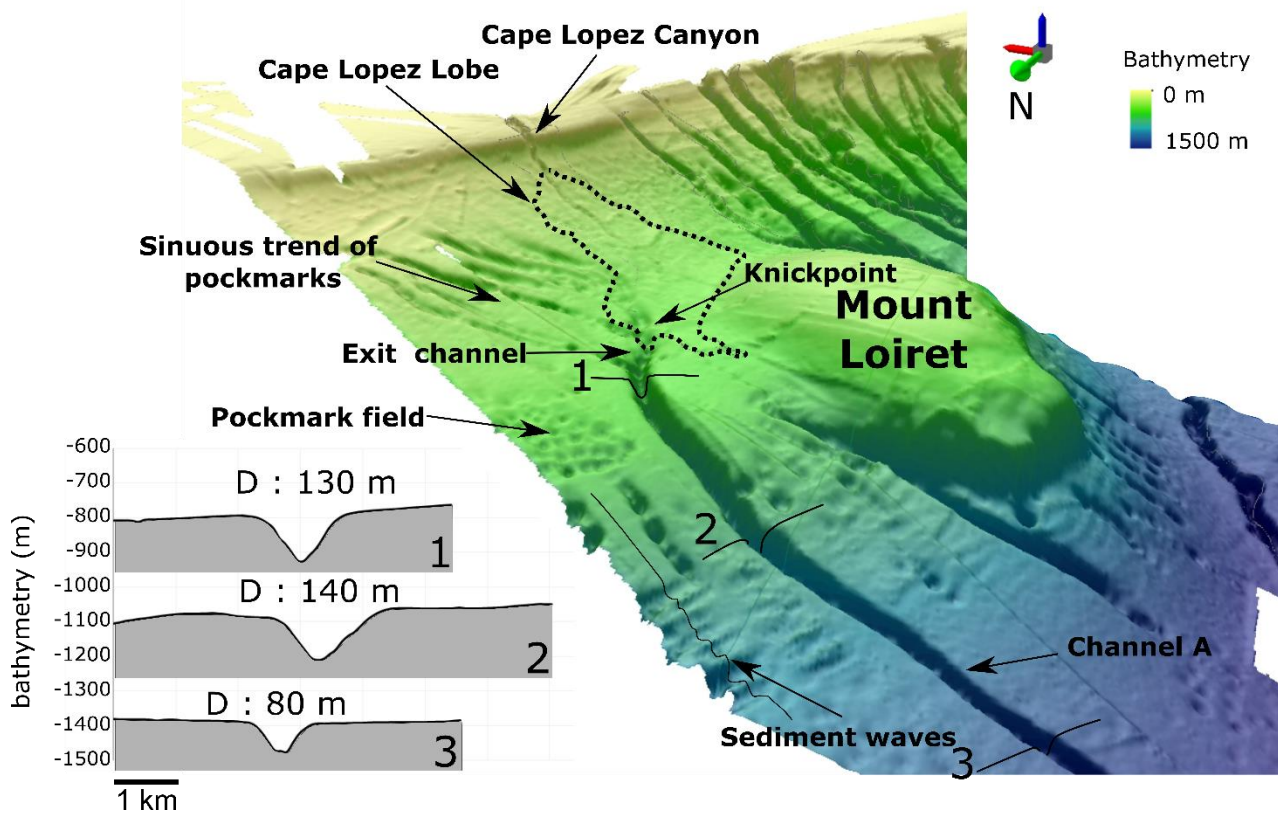
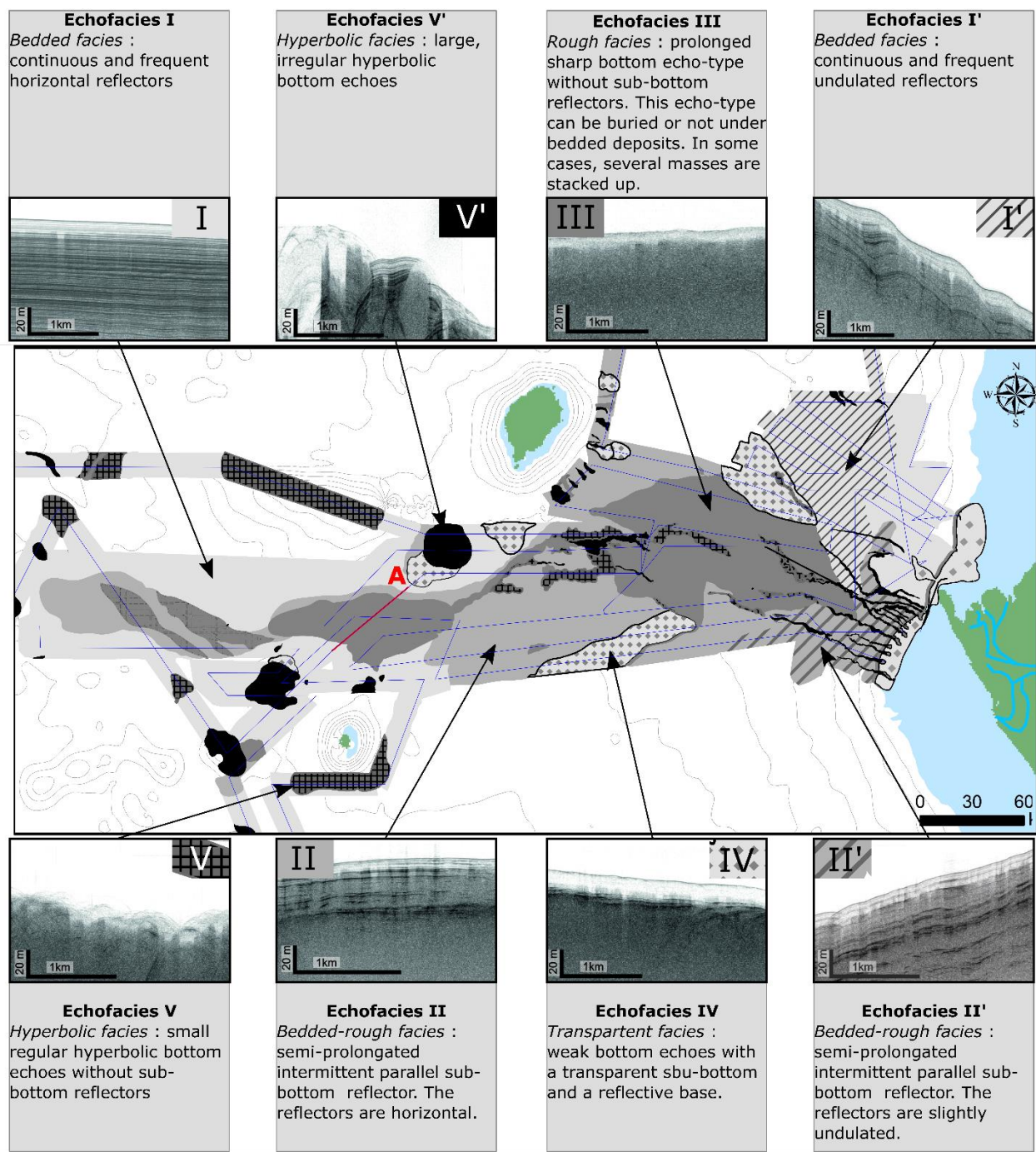


Figure 10: a) Three-dimensional representation of the Cape Lopez, Canyon, Cape Lopez Lobe and Channel A, b) three transverse profiles of Channel A. (Vertical exaggeration: 15).

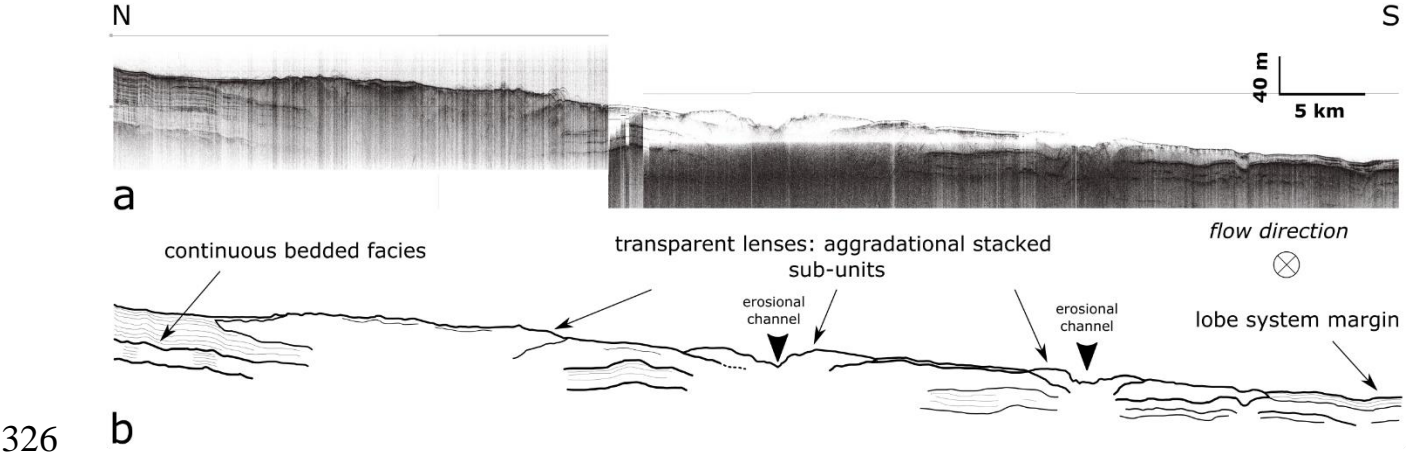
307 **4.3 Echofacies classification**



308
309 **Figure 11: Echofacies map of the Ogooue Fan. Eight shades of grey represent the specific echofacies.**

310 The main echofacies have been discriminated on the profiles based on amplitude,
311 frequency and geometry of the reflections (Figure 11). They have been grouped into
312 five main classes: (I) bedded, (II) bedded-rough, (III) rough, (IV) transparent and (V)
313 hyperbolic. Most transitions between echofacies are gradual.

314 The echofacies of the edge of the Gabonese shelf consists of transparent echofacies IV
 315 (Figure 11). North of the Mount Loiret, the continental slope presents bedded echofacies
 316 I. At 1,500 m, which corresponds to an increase in the slope gradient, echofacies
 317 transforms into echofacies I'. South of Mount Loiret, echofacies II and II' dominate on
 318 the continental slope.
 319 The echomapping of the continental rise reveals the presence of different facies. The
 320 central part, just upstream of the mid-system valley, is characterized by rough
 321 echofacies III. Some large channels are marked by hyperbolic facies. South of the mid-
 322 system valley, facies II dominates. Echofacies IV is present in two main areas on the
 323 continental rise where they respectively form two lobe-shaped zones: one on the
 324 northern part, following the limits of the high-reflectivity area located at the mouth of
 325 channel A; the second in the southern part of the system in association with channel F.



326 **b**
 327 **Figure 12: a) Transverse 3.5 kHz very-high resolution seismic line and b) line drawing in the upper distal lobe area,**
 328 **see Figure 11 for location of the line.**

329 In the abyssal plain, the area of the elongated tongue noticeable on the backscatter data
 330 presents different echofacies. Based on the 3.5 kHz profiles, it can be subdivided into
 331 two main domains. The upstream part, at the outlet of the mid-system valley, is
 332 characterized by multiple aggradational stacked transparent sub-units from 10 to
 333 30 meters thick are visible on the seismic lines (Figure 12). The downstream part
 334 presents is characterized by echofacies (II) associated with hyperbolic echofacies (V).
 335 On the edge of this tongue, high-penetration bedded facies (I) is dominant. Facies V'
 336 forms some patches on the seafloor and correspond to seafloor mounts.

Facies V and IV are also present and form lenses around the island of Sao-Tomé and Annobon.

Based on previous studies and core samples, we speculate the following links between echofacies, type of sediments and associated depositional processes:

- Bedded facies (I, I') are commonly associated with alternating sandy and silty beds (Damuth, 1975, 1980a; Pratson and Laine, 1989; Pratson and Coakley, 1996; Loncke et al., 2009) or with hemipelagic sedimentation when associated with very low reflectivity this is confirmed by facies description of cores KC16 and KC02 (Gaullier and Bellaiche, 1998).

- Rough and bedded-rough facies (II, II', III), as described in Loncke et al. 2009, are attributed to coarse-grained turbidite (Damuth, 1975; Damuth and Hayes, 1977). Damuth and Hayes (1977) have shown that a quantitative relationship exists between the relative abundance of coarse sediment in the upper few meters of the seafloor and the roughness of the echo-types. Rough echofacies characterized areas that contain the highest concentrations of coarse grains, like lobe areas, whereas bedded-rough facies contain little coarse sediments. Core KC10 and KC15, collected in an area of facies II, indicates the alternation of clayey and sandy layers but with a predominance of fine-grained sediments (Figure 5).

- Transparent facies (IV) commonly corresponds to structureless deposits due to mass-flow processes such as debris flows (Embley, 1976; Jacobi, 1976; Damuth, 1980a, 1980b, 1994) but it can also characterize basinal fine-grained turbidites (Cita et al., 1984; Tripsanas et al., 2002). In this study transparent facies is also associated with fine-grained, structureless, terrigenous sedimentation of the shelf (Core KC18).

- Hyperbolic facies (V, V') is linked to the degree of roughness of the seafloor topography. Large, irregular hyperbolae (V') are generally associated with abrupt topographies such as seamounts or canyons and deep channels. Small regular hyperbolae (V) are commonly associated with deposits generated by debris-flow (Damuth, 1980a, b, 1994).

366 **5 Interpretation and discussion**

367 **5.1 Sedimentary processes along the fan**

368 The Ogooue Fan could be classified as a delta-fed passive margin deep-sea submarine
369 fan according to Reading and Richards (1994). However, analysis of sub-surface data
370 (bathymetry, acoustic imagery and 3.5 kHz echocharacters) reveals a great variability
371 of sediment processes in the different domains of the margin, controlled by variations
372 in slope gradient and the presence of seamounts (Figure 13a).

373

374

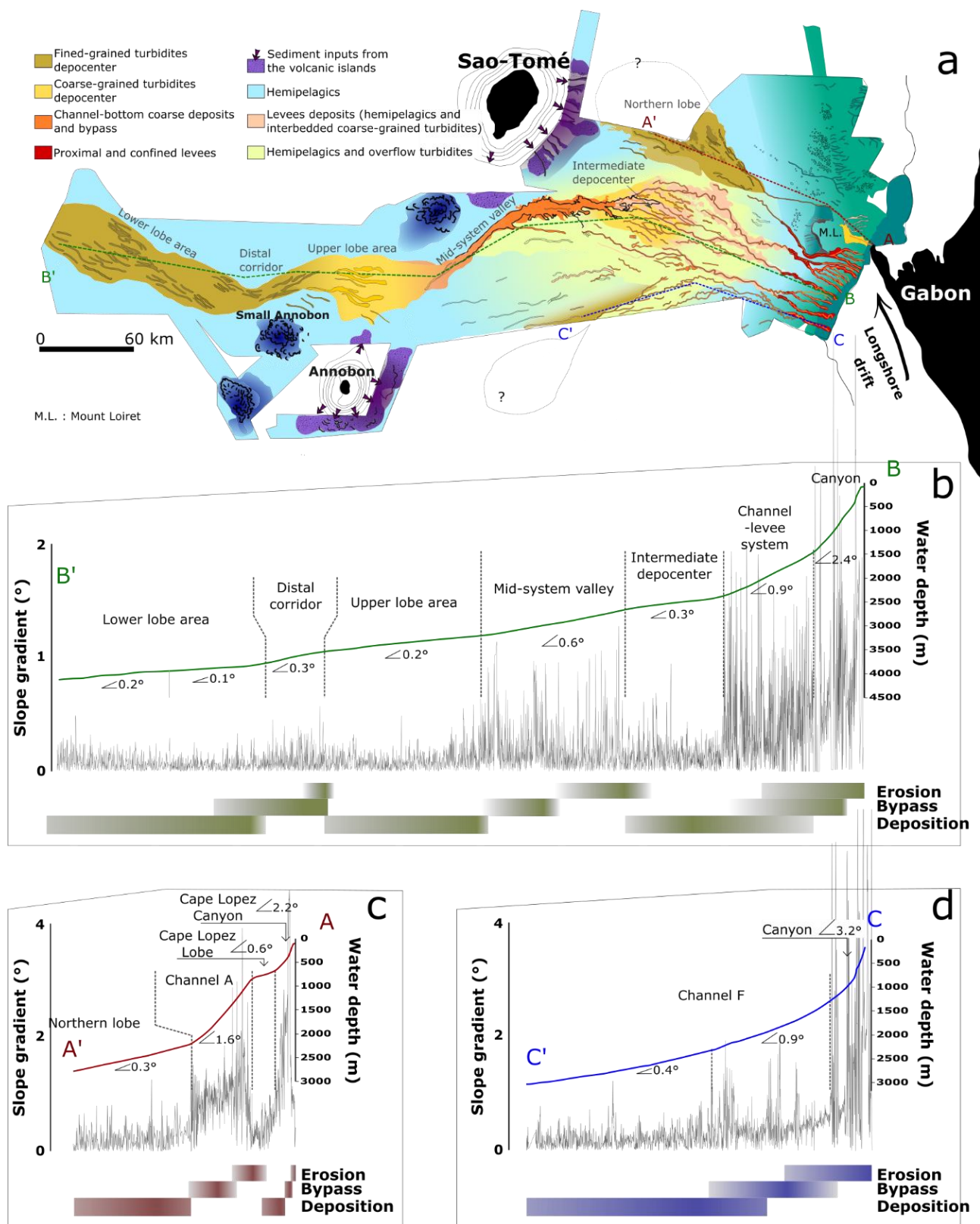


Figure 13: a) Synthetic map showing the architecture and the recent sedimentary processes of the Ogooue Fan determined by imagery and echofacies mapping; b) c) and d) Longitudinal profiles from the bathymetric data along the central, northern and southern part of the Ogooue Fan and slope gradient (in degree, measured every 100m). The differences in slope gradient along the transects are associated with the main sedimentary processes encountered along the slope.

5.1.1 Upslope area and canyons system

Cores collected in the upslope area (KC18 and KC17) show mostly hemipelagic sediments with a very low carbonate content. This reflects significant detrital flux associated with proximity to the Ogooue platform and the influence of the Ogooue river plume. Erosional processes are also active on the upper part of the slope as indicated by the presence of numerous tributary canyons (Figure 3). Based on the comparison of the canyon depths, widths and head positions, we observe the existence of two types of canyons as described in Jobe et al. (2011) along the Equatorial Guinea margin. The canyons presenting a deep (> hundreds of meters deep) “V” shape and which indent the shelf edge are type I canyons (*sensu* Jobe et al., 2011), whereas the shallower canyons (<100 m deep) with a “U” shape and which do not indent the shelf are type II canyons (*sensu* Jobe et al., 2011). The difference between these two types of canyons indicates different initiation and depositional processes. Type I are commonly associated with high sediment supply and the canyons initiation and morphology are controlled by frequent sand-rich erosive turbidity currents (Field and Gardner, 1990; Pratson et al., 1994; Pratson and Coakley, 1996; Weaver et al., 2000; Bertoni and Cartwright, 2005; Jobe et al., 2011). Core KC19 collected down of a type I canyon shows two several meters-thick sandy successions corresponding to top-cut-out Bouma sequences (Ta) interbedded with the upper slope hemipelagites. These sandy turbidites, which are the thickest sand beds recorded in all the cores (Figure 6), indicate the occurrence of high-density turbidity currents flowing down this canyon. In contrast, Type II canyons are found in areas of low sediment supply. Their initiation is attributed to retrogressive sediment failures and subsequent headward erosion (Shepard, 1981; Twichell and Roberts, 1982; Stanley and Moore, 1983). The evolution of these canyons is controlled by fine-grained sedimentation: hemipelagic deposition and dilute turbidity currents that can be carried over the shelf into the canyon heads. These sedimentary processes do not cause significant erosion in the canyons (Thornton, 1984).

North of the Mount Loiret, the fine-grained sedimentation has completely infilled several type II canyons. The fluid migration from the previously deposited coarse-

grained sediments inside the paleo-canyons has created sinuous trains of pockmarks. These pockmarks have been previously described in Pilcher and Argent (2007). Variations in the localisation of coarse-grained sediment supplies play a key role on the development of the two types of canyons. Along the central Gabonese shelf, the very recent development of the Mandji Island 3,000 years BP (Giresse and Odin, 1973; Lebigre, 1983) concentrated most of the coarse sediments near the Cape Lopez and favoured the construction of the presently active Cape Lopez Type I canyon (Biscara et al., 2013).

5.1.2 Channels system

The transition from deep canyons to sinuous channels with levees is related to a decrease in slope gradient from the continental slope ($> 2^\circ$) to the continental rise ($< 1^\circ$) that slows turbidity currents and reduces their erosional power. The external levees of the four central channels (B, C, D and E in Figure 2) show high reflectivity compared to the surrounding seafloor which indicates a different sedimentological nature. This suggests that deposition occurs on the low-developed external levees (25 m maximum levees height for channel D; Figure 7) due to turbidity currents overflows. External levee deposits have been sampled by core KC13, which shows numerous turbidites made up of centimeter-thick, normally graded, parallel or ripple cross-laminated of silt and fine sands (Figure 5). In their axial part, these channels are mainly erosive (Normark et al., 1993) as indicated by their deep incision in the seafloor: average 70 m deep for channel D and 90 m deep for channel A; (Figure 7 and Figure 10) below the associated levees, when present. This feature is similar to the modern Congo Channel (Babonneau et al., 2002) and is opposed to the morphology of aggrading channels (such as the Amazon Channel) where the thalweg is perched above the base of the levees system (Damuth, 1995). This entrenched morphology prevents extensive overflow of turbidity currents and is the probable cause of low development of external levees and limits channel by avulsion. It has been proposed for the Congo Channel that the entrenched morphology of the channel confines the flow and maintains a high velocity. The high velocity of the

438 flow enables the sediments to be transported to very distant areas (Babonneau et al.,
439 2002).

440 Several studies have documented that sinuosity of submarine channels increases with
441 time (Peakall et al., 2000; Babonneau et al., 2002; Deptuck et al., 2003, 2007; Kolla,
442 2007). The sinuous upper parts of the channels ($1.3 < \text{sinuosity} < 1.75$ for channel D;
443 Figure 7C) have consequently undergone a long history whereas the distal straighter
444 parts of the channels are in a more immature stage. Moreover, the height of the external
445 levees and the depth of the channels both decrease in the lower parts of the channel
446 system (Figure 7). These morphological changes are due to a slope gradient decrease
447 ($< 0.5^\circ$ from transect 6 along channel D; Figure 7) that progressively slows down the
448 flow velocity and reduces the erosional power of the turbidity current. Simultaneously,
449 deposition of fine particles by spilling of the upper part of the flow on the external levees
450 leads to a progressive decrease of the fine-grained fraction transported by the
451 channelized flows (Normark et al., 1993; Peakall et al., 2000).

452 At 2,200 m water depth, the appearance of numerous erosional features such as isolated
453 and amalgamated spoon-shaped scours (Figure 8 C1), erosional lineations and
454 subsidiary channels with limited surface expression (10-20 m deep, Figure 8 B2, B3)
455 are characteristic of the channel lobe transition zone (Figure 8) (Kenyon et al., 1995;
456 Wynn et al., 2007; Jegou et al., 2008; Mulder and Etienne, 2010). The appearance of
457 these features correlates with a second abrupt decrease in slope gradient (from 0.9° to
458 0.3°) and with the transition from bedded echofacies with low penetration to rough
459 echofacies indicating a change in the sedimentary process and suggest a high sand/mud
460 ratio. This area corresponds to deposition by spreading flows in an unchanneled area
461 referred as the intermediate depocenter in Figure 13 and covering area surface of ca.
462 4,250 km². However, the low penetration of the 3.5 kHz echosounder and the limited
463 number of seismic lines in this area did not allow a more detailed interpretation of the
464 sedimentary processes in this part of the system.

5.1.3 Mid-system valley and distal lobe complexes

The presence of a steeper slope downslope of the intermediate depocenter (0.6°) led to the incision of the multi-sourced mid-system valley, which acts as an outlet channel for turbidity currents that are energetic enough to travel through the flatter depositional area (Figure 13b). The numerous erosional scars present in the upstream part of the valley suggest that this section has migrated upstream by retrogressive erosion, whereas the downstream part appears more stable with a straighter pathway and steeper flanks, these features being similar to the Tanzania Channel described by Bourget et al. (2008). According to the available bathymetric data, the volume of sediment removed from the mid-system valley is between 8 and 10 km³. The pathway of the valley seems to be controlled by the seafloor topography as the valley deviates near the rocky seamount located west of Sao-Tomé. This large mid-system valley delivers sediments to the lower fan.

At the outlet of the mid-system valley, the echofacies shows an area mainly characterized by rough echofacies (III) forming stacked lenses. This organization is characteristic of sandy lobes deposits (Kenyon et al., 1995; Piper and Normark, 2001). This area, referred as the upper lobe area in Figure 13, constitutes the main lobe complex (*sensu* Prélat and Hodgson, 2013) of the Ogooue Fan. Core KC11 shows that coarse-grained turbidity currents are deposited in the proximal part of the lobe complex. The abrupt transitions between erosional/bypass and depositional behavior observed notably at the mouth of the mid-system valley is the result of hydraulic jumps affecting flows when they become unconfined between channel sides and spread laterally (Komar, 1971; Garcia and Parker, 1989). According to the seismic data, the depositional area of the lobe complex is ~ 100 km long, reaches ~ 40 km in width, spreads over 2,860 km² and reaches up to 40 m in thickness. The transparent lenses are interpreted as lobes: they seem to be bounded by erosive bases and separated vertically by fine-grained units (Mulder and Etienne, 2010; Prélat and Hodgson, 2013). Some incisions (< 15 m deep) are imaged on the top surface of the lobes; two of them are visible in Figure 12. The area where incisions are present is interpreted as the channelized part of the lobe

complex. This lobe area presents a gentle slope (0.3°) oriented north-south, suggesting that topographic compensation would shift future lobe deposition southward. However, the few numbers of seismic lines do not allow the precise internal geometry and the timing of the construction of the different lobe units.

This depositional area is not the distalmost part of the Ogooue Fan. West of this lobe, evidences of active sedimentation are visible on the reflectivity map (Figure 2, Figure 4). The reflectivity map shows high-backscatter finger-shape structures suggesting pathways of gravity flows (Figure 2b, detail A). These lineations (< 10 m deep) are concentrated in a 20 km wide corridor just west of the lobe area and then form a wider area extending up to 550 km offshore the Ogooue Delta. This part of the system follows the same pattern as the one previously described between the intermediate depocenter and the upper lobe area (Figure 13b). The corridor appears on a segment of steeper slope (0.3°) just at the downslope end of the upper lobe area (0.2°). This corridor, which disappears when the slope becomes gentler (0.1°), is certainly dominated by sediment bypass (*sensu* Stevenson et al., 2015). Core KC15, located downstream of this corridor in the lower lobe area, is composed of very thin silty turbidites corresponding to the upper parts of the Bouma sequence interbedded with hemipelagic deposits. The upper lobe acts as a trap for the basal sand-rich parts of gravity flows and the lower lobe area receive only the upper part of the flows, which is composed of fine-grained sediments. The spatial distribution of facies suggests a filling of successive depocenters with a downslope decrease of the coarse-grained sediment proportion (Figure 6).

Considering the sedimentary facies of core KC15 located downstream this corridor, we can assume that this corridor was formed by the repeated spill-over of the fine-grained top of turbidity currents over the upper lobe area. This architecture suggests that this corridor. On the most distal segment with a very low slope gradient (0.1 - 0.2°) sediment deposition dominates.

520 **5.1.4 Isolated systems**

521 On the northern part of the slope, the isolated system composed of the Cape Lopez
522 Canyon, Cape Lopez intraslope lobe, channel A and northern lobe follows the same
523 pattern (Figure 13c). The Cape Lopez intraslope lobe occupies a small confined basin,
524 6 km wide and 16 km long and covers an area of 106 km². This lobe appears very similar
525 with the “X fan” described in Jobe et al. (2017) on the Niger Delta slope (8 km x 8 km,
526 76 km²) and is in the same size range as the intraslope complexes studied in the Karoo
527 Basin by Spychala et al. (2015) (6-10 km wide and 15-25 km). The two successive
528 depositional areas, composed by the Cape Lopez lobe and the northern lobe, are located
529 on areas with a low slope gradient (0.6-0.3°) whereas erosion and sediment bypass
530 dominate on segments of steeper slope gradient (1.6°). The high slope gradient between
531 the two depositional areas favored the construction of a straight deeply entrenched
532 channel (>100 m deep near the knickpoints) without levee (Figure 7b) instead of a large
533 valley similar to the central mid-system valley.

534 In the southern part of the fan, channel F transports sediments southward (Figure 13d).
535 At 2,200 m water depth, a transparent echofacies appears associated with the pathway
536 of this channel. This echofacies suggests that sediment transported by this channel might
537 be partly deposited in this area by turbidity current overflow. This channel might also
538 be associated with a depositional lobe; however, the area covered by the MOCOSSED
539 survey does not allow us to image it.

540 **5.2 The Ogooue Fan among other complex slope fans**

541 The Ogooue Fan develops on a stepped slope (Prather, 2003) which creates a succession
542 of depositional areas on segments with gentle slope (referred as ‘steps’ in Smith (2004))
543 and segments of steeper slope (“ramps” in Smith, 2004) associated with erosion or
544 sediment bypass (Figure 13) (Demyttenaere et al., 2000; Deptuck et al., 2012; O’Byrne
545 et al., 2004; Smith, 2004). The depositional behavior in these systems is guided by an
546 equilibrium profile of the system that forms preferential areas of sedimentation or
547 erosion (Komar, 1971; Ferry et al., 2005). As described in the conceptual model of

O'Byrne et al. (2004), erosion is favored where local gradient increases, the eroded sediments being delivered downstream resulting in a local increase in sediment load (O'Byrne et al., 2004; Gee and Gawthorpe, 2006; Deptuck et al., 2012). This kind of fan geometry is common along the West African margin where abrupt changes in slope gradient and complex seafloor morphology are inherited from salt tectonic movement (Pirmez et al., 2000; Ferry et al., 2005; Gee and Gawthorpe, 2006; Gee et al., 2007). Deptuck et al. (2012) has described the influence of stepped slope on sedimentary processes along the western Niger Delta. They showed that differences of slope gradient between ramps (0.8° to 2.1°) and steps (0.3° to 1.1°) induce the transition from vertical incision and sediment removal to preferential sediment accumulation (Deptuck et al., 2007; Deptuck, 2012). Gradient changes along the Gabonese margin are however lower than the ones reported in Deptuck et al. (2012) and variation in slope gradient of 0.2° appears to be enough to modify sedimentary processes. The impact of subtle changes of slope gradients has already been highlighted by studies of the Karoo basin (Van der Merwe et al., 2014; Spychala et al., 2015; Brooks et al., 2018) and Moroccan margin where sedimentary processes are controlled by very subtle gradient changes ($<0.1^{\circ}$) (Stevenson et al., 2013; Wynn et al., 2012).

Moreover in the modern Ogooue Fan, the presence of several bathymetric highs including the volcanic islands of the CVL and the Mount Loiret acts as obstacles for the flows and creates a more complex slope profile. Such topographic highs are not present in the Congo and Niger systems. The bathymetric highs on the Ogooue fan area induce a lateral shift of the pathways of different channels as well as the pathway of the mid-system valley and form several downslope depositional lobes such as the Cape Lopez lobe that is constrained by the presence of the Mount Loiret. Several complex-slope systems have already been described in the literature with slope complexity due to salt-related deformations (e.g. Gulf of Mexico (Prather et al., 1998; Beaubouef and Friedmann, 2000), offshore Angola (Hay, 2012) or basin thrusting (offshore Brunei; McGilvery and Cook, 2003, Markan margin; Bourget et al., 2010). For these systems, the slope evolves rapidly, and sedimentation and erosion are unlikely to establish an

equilibrium profile. In contrast, the Gabonese margin reached a mature evolutionary stage with salt diapir piercement rate much lower than deposition rate and thus no conspicuous effect of salt tectonics on the deposition of overburden sediment (Chen et al., 2007). Sedimentation and erosion certainly dominate the short-term evolution of the slope. The Ogooue Fan appears to be much more similar to the morphology of the Northwest African margin where the Madeira, the Canary and the Cape Verde islands create a complex slope morphology along the Moroccan and Mauritanian margin (Masson, 1994; Wynn et al., 2000, 2002, 2012).

6 Conclusions

This study provides the first data on the morphology of the recent Ogooue Deep-sea fan and interpretations on sedimentary processes occurring in this environment. The Gabonese margin presents a pelagic/hemipelagic background sedimentation overprinted by downslope gravity flows. The fan is made up of various architectural elements and consists of both constructional and erosional sections. The pattern of sedimentation on the margin is controlled by subtle slope gradient changes ($< 0.3^\circ$). The long-term interaction between gravity flows and the seafloor topography has induced the construction of successive depocenters and sediment bypass areas. The gravity flows have modified the topography according to a theoretical equilibrium profile, eroding the seafloor where slopes are steeper than the theoretical equilibrium profiles and depositing sediments when slopes are gentler than the theoretical equilibrium profile. Three successive main sediment depocenters have been identified along a longitudinal profile. They are associated with three areas of low slope gradient (0.3° - 0.2°). The two updip deposition areas – the intermediate depocenter and the upper lobe area – have recorded coarse-grained sedimentation and are connected by a well-developed large mid-system valley measuring 100 km long and located on a steeper slope segment (0.6°). The distalmost depocenter – the lower lobe area - receive only the fine-grained portion of the sediment load that has bypassed the more proximal deposit areas. Sedimentation on this margin is made more complex by the presence of several volcanic islands and

seamounts that constrain the gravity flows. The presence on the slope of the Mount Loiret has caused the formation of an isolated system composed of the Cape Lopez Canyon and lobe, which continues downstream by the Northern Lobe area.

7 Acknowledgments

We thank the SHOM (hydrological and oceanographic marine service) for the data, the ‘ARTEMIS’ technical platform for radiocarbon age dating. We are also grateful to EPOC technicians and engineers: I. Billy, P. Lebleu, O. Ther and L. Rossignol for the data acquisition. J Covault, P. Haugton and D.M. Hodgson are thanked for their constructive and helpful reviews.

8 References

- Amy, L.A., Kneller, B.C., McCaffrey, W.D.: Facies architecture of the Grès de Peïra Cava, SE France: landward stacking patterns in ponded turbiditic basins. *J. Geol. Soc.* 164, 143–162. <https://doi.org/10.1144/0016-76492005-019>, 2007.
- Anka, Z., Séranne, M., Lopez, M., Scheck-Wenderoth, M., Savoye, B.: The long-term evolution of the Congo deep-sea fan: A basin-wide view of the interaction between a giant submarine fan and a mature passive margin (ZaiAngo project). *Tectonophysics* 470, 42–56. <https://doi.org/10.1016/j.tecto.2008.04.009>, 2009.
- Babonneau, N., Savoye, B., Cremer, M., Klein, B.: Morphology and architecture of the present canyon and channel system of the Zaire deep-sea fan. *Mar. Pet. Geol.* 19, 445–467. [https://doi.org/10.1016/S0264-8172\(02\)00009-0](https://doi.org/10.1016/S0264-8172(02)00009-0), 2002.
- Barfod, D.N., Fitton, J.G.: Pleistocene volcanism on São Tomé, Gulf of Guinea, West Africa. *Quat. Geochronol.* 21, 77–89. <https://doi.org/10.1016/j.quageo.2012.11.006>, 2014.
- Beaubouef, R.T., Friedmann, S.J.: High resolution seismic/sequence stratigraphic framework for the evolution of Pleistocene intra slope basins, western Gulf of Mexico: depositional models and reservoir analogs., in: *Deepwater Reservoirs of the World*. Presented at the SEPM, 20th Annual Research Conference, pp. 40–60, 2000.
- Bertoni, C., Cartwright, J.: 3D seismic analysis of slope-confined canyons from the Plio-Pleistocene of the Ebro Continental Margin (Western Mediterranean). *Basin Res.* 17, 43–62. <https://doi.org/10.1111/j.1365-2117.2005.00254.x>, 2005.
- Biscara, L., Mulder, T., Hanquiez, V., Marieu, V., Crespin, J.-P., Braccini, E., Garlan, T.: Morphological evolution of Cap Lopez Canyon (Gabon): Illustration of lateral

638 migration processes of a submarine canyon. *Mar. Geol.* 340, 49–56.
639 <https://doi.org/10.1016/j.margeo.2013.04.014>, 2013.

640 Biscara, L., Mulder, T., Martinez, P., Baudin, F., Etcheber, H., Jouanneau, J.-M.,
641 Garlan, T.: Transport of terrestrial organic matter in the Ogooué deep sea turbidite
642 system (Gabon). *Mar. Pet. Geol.* 28, 1061–1072.
643 <https://doi.org/10.1016/j.marpetgeo.2010.12.002>, 2011.

644 Bouma, A.H., Treadwell, T.K.: Deep-sea dune-like features. *Mar. Geol.* 19, M53–M59.
645 [https://doi.org/10.1016/0025-3227\(75\)90078-X](https://doi.org/10.1016/0025-3227(75)90078-X), 1975.

646 Bourget, J., Zaragosi, S., Ellouz-Zimmermann, S., Ducassou, E., Prins, M.A., Garlan,
647 T., Lanfumey, V., Schneider, J.-L., Rouillard, P., Giraudeau, J.: Highstand vs.
648 lowstand turbidite system growth in the Makran active margin: Imprints of high-
649 frequency external controls on sediment delivery mechanisms to deep water
650 systems. *Mar. Geol.* 274, 187–208.
651 <https://doi.org/10.1016/j.margeo.2010.04.005>, 2010.

652 Bourget, J., Zaragosi, S., Garlan, T., Gabelotaud, I., Guyomard, P., Dennielou, B.,
653 Ellouz-Zimmermann, N., Schneider, J.: Discovery of a giant deep-sea valley in
654 the Indian Ocean, off eastern Africa: The Tanzania channel. *Mar. Geol.* 255, 179–
655 185. <https://doi.org/10.1016/j.margeo.2008.09.002>, 2008.

656 Bourgoïn, J., Reyre, D., Magloire, P., Krichewsky, M.: Les canyons sous-marins du cap
657 Lopez (Gabon). *Cah Ocean.* 6, 372–387, 1963.

658 Brooks, H.L., Hodgson, D.M., Brunt, R.L., Peakall, J., Poyatos-Moré, M., Flint, S.S.:
659 Disconnected submarine lobes as a record of stepped slope evolution over
660 multiple sea-level cycles. *Geosphere* 14, 1753–1779.
661 <https://doi.org/10.1130/GES01618.1>, 2018.

662 Cameron, N.R., White, K.: Exploration Opportunities in Offshore Deepwater Africa.
663 IBC ‘Oil Gas Dev. West Afr. Lond. UK, 1999.

664 Chen, J.-C., Lo, C.Y., Lee, Y.T., Huang, S.W., Chou, P.C., Yu, H.S., Yang, T.F., Wang,
665 Y.S., Chung, S.H.: Mineralogy and chemistry of cored sediments from active
666 margin off southwestern Taiwan. *Geochem. J.* 41, 303–321, 2007.

667 Cita, M.B., Beghi, C., Camerlenghi, A., Kastens, K.A., McCoy, F.W., Nosetto, A.,
668 Parisi, E., Scolari, F., Tomadin, L.: Turbidites and megaturbidites from the
669 Herodotus abyssal plain (eastern Mediterranean) unrelated to seismic events.
670 *Mar. Geol.* 55, 79–101. [https://doi.org/10.1016/0025-3227\(84\)90134-8](https://doi.org/10.1016/0025-3227(84)90134-8), 1984.

671 Clift, P., Gaedicke, C.: Accelerated mass flux to the Arabian Sea during the middle to
672 late Miocene. *Geology* 30, 207. [https://doi.org/10.1130/0091-7613\(2002\)030<0207:AMFTTA>2.0.CO;2](https://doi.org/10.1130/0091-7613(2002)030<0207:AMFTTA>2.0.CO;2), 2002

673 Covault, J.A., Romans, B.W., Fildani, A., McGann, M., Graham, S.A.: Rapid Climatic Signal Propagation from
674 Source to Sink in a Southern California Sediment-Routing System. *J. Geol.* 118,
675 247–259. <https://doi.org/10.1086/651539>, 2010.

676
677 Covault, J.A., Romans, B.W., Graham, S.A., Fildani, A., Hilley, G.E.: Terrestrial source
678 to deep-sea sink sediment budgets at high and low sea levels: Insights from
679 tectonically active Southern California. *Geology* 39, 619–622.
680 <https://doi.org/10.1130/G31801.1>, 2011.

- Covault, J.A., Shelef, E., Traer, M., Hubbard, S.M., Romans, B.W., Fildani, A.: Deep-water channel run-out length: Insights from seafloor geomorphology. *Journal of Sedimentary Research* 82, 1, 21–36, 2012.
- Damuth, J.: The Amazon-HARP Fan Model: Facies Distributions in Mud-Rich Deep-Sea Fans Based on Systematic Coring of Architectural Elements of Amazon Fan, 1995.
- Damuth, J.E.: Neogene gravity tectonics and depositional processes on the deep Niger Delta continental margin. *Mar. Pet. Geol.* 11, 320–346. [https://doi.org/10.1016/0264-8172\(94\)90053-1](https://doi.org/10.1016/0264-8172(94)90053-1), 1994.
- Damuth, J.E.: Use of high-frequency (3.5–12 kHz) echograms in the study of near-bottom sedimentation processes in the deep-sea: a review. *Mar. Geol.* 38, 51–75, 1980a.
- Damuth, J.E.: Quaternary sedimentation processes in the South China Basin as revealed by echo-character mapping and piston-core studies, in: Hayes, D.E. (Ed.), *Geophysical Monograph Series*. American Geophysical Union, Washington, D. C., pp. 105–125. <https://doi.org/10.1029/GM023p0105>, 1980b.
- Damuth, J.E.: Echo character of the western equatorial Atlantic floor and its relationship to the dispersal and distribution of terrigenous sediments. *Mar. Geol.* 18, 17–45. [https://doi.org/10.1016/0025-3227\(75\)90047-X](https://doi.org/10.1016/0025-3227(75)90047-X), 1975.
- Damuth, J.E., Embley, R.W.: Upslope flow of turbidity currents on the northwest flank of the Ceara Rise: western Equatorial Atlantic*. *Sedimentology* 26, 825–834. <https://doi.org/10.1111/j.1365-3091.1979.tb00975.x>, 1979.
- Damuth, J.E., Hayes, D.E.: Echo character of the East Brazilian continental margin and its relationship to sedimentary processes. *Mar. Geol.* 24, 73–95. [https://doi.org/10.1016/0025-3227\(77\)90002-0](https://doi.org/10.1016/0025-3227(77)90002-0), 1977.
- Demyttenaere, R., Tromp, J.P., Ibrahim, A., Allman-Ward, P.: Brunei Deep Water Exploration: From Sea Floor Images and Shallow Seismic Analogues to Depositional Models in a Slope Turbidite Setting, in: Weimer, P. (Ed.), *Deep-Water Reservoirs of the World: 20th Annual. Society of economic palaeontologists and mineralogists*, pp. 304–317. <https://doi.org/10.5724/gcs.00.20>, 2000.
- Deptuck, M.E.: Pleistocene Seascape Evolution Above A “Simple” Stepped Slope—Western Niger Delta, in: Prather, B.E., Deptuck, M.E., Mohrig, D., Van Hoorn, B., Wynn, R.B. (Eds.), *Application of the Principles of Seismic Geomorphology to Continental-Slope and Base-of-Slope Systems: Case Studies from Seafloor and Near-Seafloor Analogues*. SEPM (Society for Sedimentary Geology). <https://doi.org/10.2110/pec.12.99>, 2012.
- Deptuck, M.E., Steffens, G.S., Barton, M., Pirmez, C.: Architecture and evolution of upper fan channel-belts on the Niger Delta slope and in the Arabian Sea. *Mar. Pet. Geol.* 20, 649–676. <https://doi.org/10.1016/j.marpetgeo.2003.01.004>, 2003.
- Deptuck, M.E., Sylvester, Z., Pirmez, C., O’Byrne, C.: Migration–aggradation history and 3-D seismic geomorphology of submarine channels in the Pleistocene Benin-

major Canyon, western Niger Delta slope. *Mar. Pet. Geol.* 24, 406–433.
<https://doi.org/10.1016/j.marpetgeo.2007.01.005>, 2007.

Déruelle, B., Ngounouno, I., Demaiffe, D.: The ‘Cameroon Hot Line’ (CHL): A unique
 example of active alkaline intraplate structure in both oceanic and continental
 lithospheres. *Comptes Rendus Geosci.* 339, 589–600.
<https://doi.org/10.1016/j.crte.2007.07.007>, 2007.

Dill, R.F., Dietz, R.S., Stewart, H.: deep-sea channels and delta of the Monterey
 submarine canyon. *Geol. Soc. Am. Bull.* 65, 191. [https://doi.org/10.1130/0016-7606\(1954\)65\[191:DCADOT\]2.0.CO;2](https://doi.org/10.1130/0016-7606(1954)65[191:DCADOT]2.0.CO;2), 1954.

Droz, L., Marsset, T., Ondras, H., Lopez, M., Savoye, B., Spy-Anderson, F.-L.:
 Architecture of an active mud-rich turbidite system: The Zaire Fan (Congo–
 Angola margin southeast Atlantic): Results from ZaAngo 1 and 2 cruises. *AAPG
 Bull.* 87, 1145–1168, 2003.

Droz, L., Rigaut, F., Cochonat, P., Tofani, R.: Morphology and recent evolution of the
 Zaire turbidite system (Gulf of Guinea). *Geol. Soc. Am. Bull.* 108, 253–269.
[https://doi.org/10.1130/0016-7606\(1996\)108<0253:MAREOT>2.3.CO;2](https://doi.org/10.1130/0016-7606(1996)108<0253:MAREOT>2.3.CO;2), 1996.

Embley, R.W.: New evidence for occurrence of debris flow deposits in the deep sea.
Geology 4, 371. [https://doi.org/10.1130/0091-7613\(1976\)4<371:NEFOOD>2.0.CO;2](https://doi.org/10.1130/0091-7613(1976)4<371:NEFOOD>2.0.CO;2), 1976.

Ferry, J.-N., Mulder, T., Parize, O., Raillard, S.: Concept of equilibrium profile in deep-
 water turbidite system: effects of local physiographic changes on the nature of
 sedimentary process and the geometries of deposits. *Geol. Soc. Lond. Spec. Publ.*
 244, 181–193. <https://doi.org/10.1144/GSL.SP.2005.244.01.11>, 2005.

Field, M.E., Gardner, J.V.: Pliocene-Pleistocene growth of the Rio Ebro margin,
 northeast Spain: A prograding-slope model. *Geol. Soc. Am. Bull.* 102, 721–733.
[https://doi.org/10.1130/0016-7606\(1990\)102<0721:PPGOTR>2.3.CO;2](https://doi.org/10.1130/0016-7606(1990)102<0721:PPGOTR>2.3.CO;2), 1990.

Fildani, A., Normark, W.R.: Late Quaternary evolution of channel and lobe complexes
 of Monterey Fan. *Mar. Geol.* 206, 199–223.
<https://doi.org/10.1016/j.margeo.2004.03.001>, 2004.

Garcia, M., Parker, G.: Experiments on hydraulic jumps in turbidity currents near a
 canyon-fan transition. *Science* 245, 393–396.
<https://doi.org/10.1126/science.245.4916.393>, 1989.

Garlan, T., Biscara, L., Guyomard, P., Le Faou, Y., Gabelotaud, I.: Rapport de la
 campagne MOCOSÉD 2010, Modèle de couches sédimentaires du Golfe de
 Guinée (Rapport de mission). SHOM, 2010.

Gaullier, V., Bellaiche, G.: Near-bottom sedimentation processes revealed by echo-
 character mapping studies, north-western Mediterranean Basin. *AAPG Bull.* 82,
 1140–1155, 1998.

Gay, A., Lopez, M., Cochonat, P., Sultan, N., Cauquil, E., Brigaud, F.: Sinuous
 pockmark belt as indicator of a shallow buried turbiditic channel on the lower
 slope of the Congo basin, West African margin. *Geol. Soc. Lond. Spec. Publ.*
 216, 173–189. <https://doi.org/10.1144/GSL.SP.2003.216.01.12>, 2003.

765 Gee, M.J.R., Gawthorpe, R.L.: Submarine channels controlled by salt tectonics:
 766 Examples from 3D seismic data offshore Angola. *Mar. Pet. Geol.* 23, 443–458.
 767 <https://doi.org/10.1016/j.marpetgeo.2006.01.002>, 2006.

768 Gee, M.J.R., Gawthorpe, R.L., Bakke, K., Friedmann, S.J.: Seismic Geomorphology
 769 and Evolution of Submarine Channels from the Angolan Continental Margin. *J.*
 770 *Sediment. Res.* 77, 433–446. <https://doi.org/10.2110/jsr.2007.042>, 2007.

771 Giresse, P.: Carte sédimentologique des fonds sous-marins du delta de l'Ogooué, 1969.
 772 Giresse, P., Odin, G.S.: Nature minéralogique et origine des glauconies du plateau
 773 continental du Gabon et du Congo. *Sedimentology* 20, 457–488, 1973.

774 Guillou, R.: MOCOSED 2010 croise, Pourquoi pas ?
 775 <https://doi.org/10.17600/10030110>, 2010.

776 Hanquiez, V., Mulder, T., Lecroart, P., Gonthier, E., Marchès, E., Voisset, M.: High
 777 resolution seafloor images in the Gulf of Cadiz, Iberian margin. *Mar. Geol.* 246,
 778 42–59. <https://doi.org/10.1016/j.margeo.2007.08.002>, 2007.

779 Hay, D.: Stratigraphic evolution of a tortuous corridor from the stepped slope of Angola,
 780 in: Prather, B.E., Deptuck, M.E., Mohrig, D., Van Hoorn, B., Wynn, R.B. (Eds.),
 781 Application of the Principles of Seismic Geomorphology to Continental-Slope
 782 and Base-of-Slope Systems: Case Studies from Seafloor and Near-Seafloor
 783 Analogues. SEPM (Society for Sedimentary Geology).
 784 <https://doi.org/10.2110/pec.12.99>, 2012.

785 Heezen, B.C., Tharp, M., Ewing, M.: The Floors of the Oceans, in: Geological Society
 786 of America Special Papers. Geological Society of America, pp. 1–126.
 787 <https://doi.org/10.1130/SPE65-p1>, 1959.

788 Jacobi, R.D.: Sediment slides on the northwestern continental margin of Africa. *Mar.*
 789 *Geol.* 22, 157–173. [https://doi.org/10.1016/0025-3227\(76\)90045-1](https://doi.org/10.1016/0025-3227(76)90045-1), 1976.

790 Jansen, J.H.F., Van Weering, T.C.E., Gieles, R., Van Iperen, J.: Middle and late
 791 Quaternary oceanography and climatology of the Zaire-Congo fan and the
 792 adjacent eastern Angola Basin. *Neth. J. Sea Res.* 17, 201–249, 1984.

793 Jegou, I., Savoye, B., Pirmez, C., Droz, L.: Channel-mouth lobe complex of the recent
 794 Amazon Fan: The missing piece. *Mar. Geol.* 252, 62–77.
 795 <https://doi.org/10.1016/j.margeo.2008.03.004>, 2008.

796 Jobe, Z.R., Lowe, D.R., Uchytel, S.J.: Two fundamentally different types of submarine
 797 canyons along the continental margin of Equatorial Guinea. *Mar. Pet. Geol.* 28,
 798 843–860. <https://doi.org/10.1016/j.marpetgeo.2010.07.012>, 2011.

799 Jobe, Z.R., Sylvester, Z., Howes, N., Pirmez, C., Parker, A., Cantelli, A., Smith, R.,
 800 Wolinsky, M.A., O'Byrne, C., Slowey, N., Prather, B.: High-resolution,
 801 millennial-scale patterns of bed compensation on a sand-rich intraslope
 802 submarine fan, western Niger Delta slope. *Geol. Soc. Am. Bull.* 129, 23–37.
 803 <https://doi.org/10.1130/B31440.1>, 2017.

804 Kane, I.A., Catterall, V., McCaffrey, W.D., Martinsen, O.J.: Submarine channel
 805 response to intrabasinal tectonics: The influence of lateral tilt. *AAPG Bull.* 94,
 806 189–219. <https://doi.org/10.1306/08180909059>, 2010.

- Kenyon, N.H., Millington, J., Droz, L., Ivanov, M.K.: Scour holes in a channel-lobe transition zone on the Rhône Cone, in: *Atlas of Deep Water Environments*. Springer, Dordrecht, pp. 212–215. https://doi.org/10.1007/978-94-011-1234-5_31, 1995.
- Kneller, B.: Beyond the turbidite paradigm: physical models for deposition of turbidites and their implications for reservoir prediction. *Geol. Soc. Lond. Spec. Publ.* 94, 31–49. <https://doi.org/10.1144/GSL.SP.1995.094.01.04>, 1995.
- Kolla, V.: A review of sinuous channel avulsion patterns in some major deep-sea fans and factors controlling them. *Mar. Pet. Geol.* 24, 450–469. <https://doi.org/10.1016/j.marpetgeo.2007.01.004>, 2007.
- Kolla, V., Coumes, F.: Morphology, Internal Structure, Seismic Stratigraphy, and Sedimentation of Indus Fan. *AAPG Bull.* 71, 650–677, 1987.
- Komar, P.D.: Hydraulic jumps in turbidity currents. *Bull. Geol. Soc. Am.* 82, 1477–1488. [https://doi.org/10.1130/0016-7606\(1971\)82\[1477:HJITC\]2.0.CO;2](https://doi.org/10.1130/0016-7606(1971)82[1477:HJITC]2.0.CO;2), 1971.
- Lebigre, J.M.: Les mangroves des rias du littoral gabonais, essai de cartographie typologique. *Rev. Bois For. Trop.*, 1983.
- Lee, D.-C., Halliday, A.N., Fitton, J.G., Poli, G.: Isotopic variations with distance and time in the volcanic islands of the Cameroon line: evidence for a mantle plume origin. *Earth Planet. Sci. Lett.* 123, 119–138. [https://doi.org/10.1016/0012-821X\(94\)90262-3](https://doi.org/10.1016/0012-821X(94)90262-3), 1994.
- Lerique, J., Barret, J., Walter, R.: Hydrographie, hydrologie, in: *Géographie et cartographie du Gabon : atlas illustré*. EDICEF, Paris, pp. 14–17, 1983.
- Loncke, L., Droz, L., Gaullier, V., Basile, C., Patriat, M., Roest, W.: Slope instabilities from echo-character mapping along the French Guiana transform margin and Demerara abyssal plain. *Mar. Pet. Geol.* 26, 711–723. <https://doi.org/10.1016/j.marpetgeo.2008.02.010>, 2009.
- Lonergan, L., Jamin, N.H., Jackson, C.A.-L., Johnson, H.D.: U-shaped slope gully systems and sediment waves on the passive margin of Gabon (West Africa). *Mar. Geol.* 337, 80–97. <https://doi.org/10.1016/j.margeo.2013.02.001>, 2013.
- Mahé, G., Lerique, J., Olivry, J.-C.: Le fleuve Ogooué au Gabon : reconstitution des débits manquants et mise en évidence de variations climatiques à l'équateur. *Hydrol Cont.* 5, 105–124, 1990.
- Masson, D.G.: Late Quaternary turbidity current pathways to the Madeira Abyssal Plain and some constraints on turbidity current mechanisms. *Basin Res.* 6, 17–33. <https://doi.org/10.1111/j.1365-2117.1994.tb00072.x>, 1994.
- Masson, D.G., Kenyon, N.H., Gardner, J.V., Field, M.E.: Monterey Fan: channel and overbank morphology, in: Pickering, K.T., Hiscott, R.N., Kenyon, N.H., Ricci Lucchi, F., Smith, R.D.A. (Eds.), *Atlas of Deep Water Environments*. Springer Netherlands, Dordrecht, pp. 74–79. https://doi.org/10.1007/978-94-011-1234-5_13, 1995.
- McGilvery, T.A., Cook, D.L.: The Influence of Local Gradients on Accommodation Space and Linked Depositional Elements Across a Stepped Slope Profile, Offshore Brunei, in: Roberts, H.R., Rosen, N.C., Fillon, R.F., Anderson, J.B.

(Eds.), Shelf Margin Deltas and Linked Down Slope Petroleum Systems: 23rd Annual. SOCIETY OF ECONOMIC PALEONTOLOGISTS AND MINERALOGISTS. <https://doi.org/10.5724/gcs.03.23>, 2003.

Menard, H.W.: Deep-Sea Channels, Topography, and Sedimentation. AAPG Bull. 39, 255, 1955.

Migeon, S., Weber, O., Faugeres, J.-C., Saint-Paul, J.: SCOPIX: A new X-ray imaging system for core analysis. Geo-Mar. Lett. 18, 251–255. <https://doi.org/10.1007/s003670050076>, 1998.

Mignard, S.L.-A., Mulder, T., Martinez, P., Charlier, K., Rossignol, L., Garlan, T.: Deep-sea terrigenous organic carbon transfer and accumulation: Impact of sea-level variations and sedimentation processes off the Ogooué River (Gabon). Mar. Pet. Geol. 85, 35–53. <https://doi.org/10.1016/j.marpetgeo.2017.04.009>, 2017.

Mougamba, R.: Chronologie et architecture des systems turbiditiques Cénozoïques du Prisme sédimentaire de l'Ogooué (Marge Nord-Gabon). Université de Lille, Lille, 1999.

Mouscardes, P.: OPTIC CONGO 2 cruise, RV Beautemps-Beaupré [www Document]. URL <http://campagnes.flotteoceanographique.fr/campagnes/5090050/fr/> (accessed 7.5.18), 2005.

Mulder, T., Alexander, J.: Abrupt change in slope causes variation in the deposit thickness of concentrated particle-driven density currents. Mar. Geol. 175, 221–235. [https://doi.org/10.1016/S0025-3227\(01\)00114-1](https://doi.org/10.1016/S0025-3227(01)00114-1), 2001.

Mulder, T., Etienne, S.: Lobes in deep-sea turbidite systems: State of the art. Sediment. Geol. 229, 75–80. <https://doi.org/10.1016/j.sedgeo.2010.06.011>, 2010.

Normark, W.R., Barnes, N.E., Coumes, F.: Rhone Deep-Sea Fan: A review. Geo-Mar. Lett. 3, 155–160. <https://doi.org/10.1007/BF02462461>, 1983.

Normark, W.R., Damuth, J.E.: Sedimentary facies and associated depositional elements of the Amazon Fan, Proceedings of the Ocean Drilling Program. Ocean Drilling Program. <https://doi.org/10.2973/odp.proc.sr.155.1997>, 1997.

Normark, W.R., Piper, D.J.W.: Initiation processes and flow evolution of turbidity currents: implications for the depositional record, in: From Shoreline to Abyss, SEPM Special Publication. pp. 207–230, 1991.

Normark, W.R., Posamentier, H., Mutti, E.: Turbidite systems: State of the art and future directions. Rev. Geophys. 31, 91–116. <https://doi.org/10.1029/93RG02832>, 1993.

O'Byrne, C., Prather, B., Pirmez, C., Steffens, G.S.: Reservoir architectural styles across stepped slope profiles: Implications for exploration, appraisal and development. Presented at the AAPG International conference, 2004.

Olausson, E.: Oxygen and carbon isotope analyses of a late quaternary core in the Zaire (Congo) fan. Neth. J. Sea Res. 17, 276–279. [https://doi.org/10.1016/0077-7579\(84\)90050-4](https://doi.org/10.1016/0077-7579(84)90050-4), 1984.

Peakall, J., McCaffrey, B., Kneller, B.: A Process Model for the Evolution, Morphology, and Architecture of Sinuous Submarine Channels. J. Sediment. Res. 70, 434–448. <https://doi.org/10.1306/2DC4091C-0E47-11D7-8643000102C1865D>, 2000.

- Pettingill, H.S., Weimer, P.: Worldwide deepwater exploration and production: Past, present, and future. *Lead. Edge* 21, 371–376. <https://doi.org/10.1190/1.1471600>, 2002.
- Pickering, K., Stow, D., Watson, M., Hiscott, R.: Deep-water facies, processes and models: a review and classification scheme for modern and ancient sediments. *Earth Sci. Rev.* 23, 75–174. [https://doi.org/10.1016/0012-8252\(86\)90001-2](https://doi.org/10.1016/0012-8252(86)90001-2), 1986.
- Pilcher, R., Argent, J.: Mega-pockmarks and linear pockmark trains on the West African continental margin. *Mar. Geol.* 244, 15–32. <https://doi.org/10.1016/j.margeo.2007.05.002>, 2007.
- Piper, D.J.W., Normark, W.R.: Processes That Initiate Turbidity Currents and Their Influence on Turbidites: A Marine Geology Perspective. *J. Sediment. Res.* 79, 347–362. <https://doi.org/10.2110/jsr.2009.046>, 2009.
- Piper, D.J.W., Normark, W.R.: Sandy fans-from Amazon to Hueneme and beyond. *AAPG Bull.* 85, 1407–1438, 2001.
- Pirmez, C., Beaubouef, R.T., Friedmann, S.J., Mohrig, D.C.: Equilibrium Profile and Baselevel in Submarine Channels: Examples from Late Pleistocene Systems and Implications for the Architecture of Deepwater Reservoirs, in: Weimer, P. (Ed.), *Deep-Water Reservoirs of the World*. <https://doi.org/10.5724/gcs.00.20>, 2000.
- Prather, B.E.: Controls on reservoir distribution, architecture and stratigraphic trapping in slope settings. *Mar. Pet. Geol.* 20, 529–545. <https://doi.org/10.1016/j.marpetgeo.2003.03.009>, 2003.
- Prather, B.E., Booth, J.R., Steffens, G.S., Craig, P.A.: Classification, Lithologic Calibration, and Stratigraphic Succession of Seismic Facies of Intraslope Basins, Deep-Water Gulf of Mexico. *AAPG Bull.* 82, 701–728, 1998.
- Prather, B.E., O’Byrne, C., Pirmez, C., Sylvester, Z.: Sediment partitioning, continental slopes and base-of-slope systems. *Basin Res.* 29, 394–416. <https://doi.org/10.1111/bre.12190>, 2017.
- Pratson, L.F., Coakley, B.J.: A model for the headward erosion of submarine canyons induced by downslope-eroding sediment flows. *Geol. Soc. Am. Bull.* 108, 225–234. [https://doi.org/10.1130/0016-7606\(1996\)108<0225:AMFTHE>2.3.CO;2](https://doi.org/10.1130/0016-7606(1996)108<0225:AMFTHE>2.3.CO;2), 1996.
- Pratson, L.F., Laine, E.P.: The relative importance of gravity-induced versus current-controlled sedimentation during the Quaternary along the Mideast U.S. outer continental margin revealed by 3.5 kHz echo character. *Mar. Geol.* 89, 87–126. [https://doi.org/10.1016/0025-3227\(89\)90029-7](https://doi.org/10.1016/0025-3227(89)90029-7), 1989.
- Pratson, L.F., Ryan, W.B.F., Mountain, G.S., Twichell, D.C.: Submarine canyon initiation by downslope-eroding sediment flows: Evidence in late Cenozoic strata on the New Jersey continental slope. *Geol. Soc. Am. Bull.* 106, 395–412. [https://doi.org/10.1130/0016-7606\(1994\)106<0395:SCIBDE>2.3.CO;2](https://doi.org/10.1130/0016-7606(1994)106<0395:SCIBDE>2.3.CO;2), 1994.
- Prélat, A., Hodgson, D.M.: The full range of turbidite bed thickness patterns in submarine lobes: controls and implications. *J. Geol. Soc.* 170, 209–214. <https://doi.org/10.1144/jgs2012-056>, 2013.

- Rasmussen, E.S.: Structural evolution and sequence formation offshore South Gabon during the Tertiary. *Tectonophysics, Dynamics of Extensional Basins and Inversion Tectonics* 266, 509–523. [https://doi.org/10.1016/S0040-1951\(96\)00236-3](https://doi.org/10.1016/S0040-1951(96)00236-3), 1996.
- Reading, H.G., Richards, M.: Turbidite systems in deep-water basin margins classified by grain size and feeder system. *AAPG Bull.* 78, 792–822, 1994.
- Reimer, P.: IntCal13 and Marine13 Radiocarbon Age Calibration Curves 0–50,000 Years cal BP. *Radiocarbon* 55, 1869–1887. https://doi.org/10.2458/azu_js_rc.55.16947, 2013.
- Salles, L., Ford, M., Joseph, P.: Characteristics of axially-sourced turbidite sedimentation on an active wedge-top basin (Annot Sandstone, SE France). *Mar. Pet. Geol.* 56, 305–323. <https://doi.org/10.1016/j.marpetgeo.2014.01.020>, 2014.
- Séranne, M., Anka, Z.: South Atlantic continental margins of Africa: A comparison of the tectonic vs climate interplay on the evolution of equatorial West Africa and SW Africa margins. *J. Afr. Earth Sci.* 43, 283–300. <https://doi.org/10.1016/j.jafrearsci.2005.07.010>, 2005.
- Séranne, M., Bruguier, O., Moussavou, M.: U-Pb single zircon grain dating of Present fluvial and Cenozoic aeolian sediments from Gabon: consequences on sediment provenance, reworking, and erosion processes on the equatorial West African margin. *Bull. Société Géologique Fr.* 179, 29–40, 2008.
- Séranne, M., Nzé Abeigne, C.-R.: Oligocene to Holocene sediment drifts and bottom currents on the slope of Gabon continental margin (West Africa). *Sediment. Geol.* 128, 179–199. [https://doi.org/10.1016/S0037-0738\(99\)00069-X](https://doi.org/10.1016/S0037-0738(99)00069-X), 1999.
- Shepard, F.P.: Submarine Canyons: Multiple Causes and Long-Time Persistence. *AAPG Bull.* 65. <https://doi.org/10.1306/03B59459-16D1-11D7-8645000102C1865D>, 1981.
- Shepard, F.P.: submarine erosion, a discussion of recent papers. *Geol. Soc. Am. Bull.* 62, 1413. [https://doi.org/10.1130/0016-7606\(1951\)62\[1413:SEADOR\]2.0.CO;2](https://doi.org/10.1130/0016-7606(1951)62[1413:SEADOR]2.0.CO;2), 1951.
- Shepard, F.P., Emery, K.O.: Submarine Topography off the California Coast: Canyons and Tectonic Interpretation, Geological Society of America Special Papers. Geological Society of America. <https://doi.org/10.1130/SPE31>, 1941.
- Smith, R.: Silled sub-basins to connected tortuous corridors: sediment distribution systems on topographically complex sub-aqueous slopes. *Geol. Soc. Lond. Spec. Publ.* 222, 23–43. <https://doi.org/10.1144/GSL.SP.2004.222.01.03>, 2004.
- Spychala, Y.T., Hodgson, D.M., Flint, S.S., Mountney, N.P.: Constraining the sedimentology and stratigraphy of submarine intraslope lobe deposits using exhumed examples from the Karoo Basin, South Africa. *Sediment. Geol.* 322, 67–81. <https://doi.org/10.1016/j.sedgeo.2015.03.013>, 2015.
- Stanley, D.J., Moore, G.T.: The Shelfbreak: Critical Interface on Continental Margins. *SEPM (Society for Sedimentary Geology)*. <https://doi.org/10.2110/pec.83.33>, 1983.

- Stevenson, C.J., Jackson, C.A.-L., Hodgson, D.M., Hubbard, S.M., Eggenhuisen, J.T.: Deep-Water Sediment Bypass. *J. Sediment. Res.* 85, 1058–1081. <https://doi.org/10.2110/jsr.2015.63>, 2015.
- Stevenson, C.J., Talling, P.J., Wynn, R.B., Masson, D.G., Hunt, J.E., Frenz, M., Akhmetzhanov, A., Cronin, B.T.: The flows that left no trace: Very large-volume turbidity currents that bypassed sediment through submarine channels without eroding the sea floor. *Mar. Pet. Geol.* 41, 186–205. <https://doi.org/10.1016/j.marpetgeo.2012.02.008>, 2013.
- Stow, D.A.V., Piper, D.J.W.: Deep-water fine-grained sediments: facies models. *Geol. Soc. Lond. Spec. Publ.* 15, 611–646. <https://doi.org/10.1144/GSL.SP.1984.015.01.38>, 1984.
- Sylvester, Z., Cantelli, A., Pirmez, C.: Stratigraphic evolution of intraslope minibasins: Insights from surface-based model. *AAPG Bull.* 99, 1099–1129. <https://doi.org/10.1306/01081514082>, 2015.
- Syvitski, J.P.M., Vörösmarty, C.J., Kettner, A.J., Green, P.: Impact of Humans on the Flux of Terrestrial Sediment to the Global Coastal Ocean. *Science* 308, 376–380. <https://doi.org/10.1126/science.1109454>, 2005.
- Thornton, S.E.: Hemipelagites and Associated Facies of Slopes and Slope Basins. *Geol. Soc. Lond. Spec. Publ.* 15, 377–394, 1984.
- Tripsanas, E.K., Phaneuf, B.A., Bryant, W.R.: Slope Instability Processes in a Complex Deepwater Environment, Bryant Canyon Area, Northwest Gulf of Mexico, in: Offshore Technology Conference. Presented at the Offshore Technology Conference, Offshore Technology Conference, Houston, Texas. <https://doi.org/10.4043/14273-MS>, 2002.
- Twichell, D.C., Roberts, D.G.: Morphology, distribution, and development of submarine canyons on the United States Atlantic continental slope between Hudson and Baltimore Canyons. *Geology* 10, 408. [https://doi.org/10.1130/0091-7613\(1982\)10<408:MDADOS>2.0.CO;2](https://doi.org/10.1130/0091-7613(1982)10<408:MDADOS>2.0.CO;2), 1982.
- Unterseh, S.: Cartographie et caractérisation du fond marin par sondeur multifaisceaux. Vandoeuvre-les-Nancy, INPL, 1999.
- Van der Merwe, W.C., Hodgson, D.M., Brunt, R.L., Flint, S.S.: Depositional architecture of sand-attached and sand-detached channel-lobe transition zones on an exhumed stepped slope mapped over a 2500 km² area. *Geosphere* 10, 1076–1093. <https://doi.org/10.1130/GES01035.1>, 2014.
- Volat, J.-L., Pastouret, L., Vergnaud-Grazzini, C.: Dissolution and carbonate fluctuations in Pleistocene deep-sea cores: A review. *Mar. Geol.* 34, 1–28. [https://doi.org/10.1016/0025-3227\(80\)90138-3](https://doi.org/10.1016/0025-3227(80)90138-3), 1980.
- Weaver, P.P.E., Wynn, R.B., Kenyon, N.H., Evans, J.: Continental margin sedimentation, with special reference to the north-east Atlantic margin: Continental slope sedimentation. *Sedimentology* 47, 239–256. <https://doi.org/10.1046/j.1365-3091.2000.0470s1239.x>, 2000.

- Wonham, J., Jayr, S., Mougamba, R., Chuilon, P.: 3D sedimentary evolution of a canyon fill (Lower Miocene-age) from the Mandorove Formation, offshore Gabon. *Mar. Pet. Geol.* 17, 175–197. [https://doi.org/10.1016/S0264-8172\(99\)00033-1](https://doi.org/10.1016/S0264-8172(99)00033-1), 2000.
- Wynn, R. B., Talling, P.J., Masson, D.G., Le Bas, T.P., Cronin, B.T., Stevenson, C.J.: The Influence of Subtle Gradient Changes on Deep-Water Gravity Flows: A Case Study From the Moroccan Turbidite System, in: Prather, B.E., Deptuck, M.E., Mohrig, D., Van Hoorn, B., Wynn, Russell B. (Eds.), *Application of the Principles of Seismic Geomorphology to Continental-Slope and Base-of-Slope Systems: Case Studies from Seafloor and Near-Seafloor Analogues*. SEPM (Society for Sedimentary Geology). <https://doi.org/10.2110/pec.12.99>, 2012.
- Wynn, R.B., Cronin, B.T., Peakall, J.: Sinuous deep-water channels: Genesis, geometry and architecture. *Mar. Pet. Geol.* 24, 341–387. <https://doi.org/10.1016/j.marpetgeo.2007.06.001>, 2007.
- Wynn, R.B., Masson, D.G., Stow, D.A., Weaver, P.P.: Turbidity current sediment waves on the submarine slopes of the western Canary Islands. *Mar. Geol.* 163, 185–198, 2000.
- Wynn, R.B., Weaver, P.P.E., Masson, D.G., Stow, D.A.V.: Turbidite depositional architecture across three interconnected deep-water basins on the north-west African margin. *Sedimentology* 49, 669–695. <https://doi.org/10.1046/j.1365-3091.2002.00471.x>, 2002.
- Zachariasse, W.J., Schmidt, R.R., Van Leeuwen, R.J.W.: Distribution of foraminifera and calcareous nannoplankton in quaternary sediments of the eastern Angola basin in response to climatic and oceanic fluctuations. *Neth. J. Sea Res.* 17, 250–275, 1984.